nature microbiology

Article

https://doi.org/10.1038/s41564-024-01794-8

Sulfated glycosaminoglycans are host epithelial cell targets of the *Candida albicans* toxin candidalysin

Received: 11 December 2023

Accepted: 23 July 2024

Published online: 16 September 2024

Check for updates

Jianfeng Lin[1], Jian Miao[2], Katherine G. Schaefer[3], Charles M. Russell[4], Robert J. Pyron[5], Fuming Zhang[6], Quynh T. Phan[1], Norma V. Solis[1], Hong Liu[1], Masato Tashiro[1,7], Jonathan S. Dordick[6], Robert J. Linhardt[6], Michael R. Yeaman[1,8,9,10], Gavin M. King[3,11], Francisco N. Barrera[4], Brian M. Peters[12,13] & Scott G. Filler[1,8,9] ✉

Candidalysin, a cytolytic peptide produced by the fungal pathogen *Candida albicans*, is a key virulence factor. However, its host cell targets remain elusive. Here we performed a genome-wide loss-of-function CRISPR screen in the TR146 human oral epithelial cell line and identified that disruption of genes (*XYLT2*, *B3GALT6* and *B3GAT3*) in glycosaminoglycan (GAG) biosynthesis conferred resistance to damage induced by candidalysin and live *C. albicans*. Surface plasmon resonance and atomic force and electron microscopy indicated that candidalysin binds to sulfated GAGs, facilitating its enrichment on the host cell surface. Adding exogenous sulfated GAGs or the analogue dextran sulfate protected cells against candidalysin-induced damage. Dextran sulfate also inhibited *C. albicans* invasion and fungal-induced epithelial cell cytokine production. In mice with vulvovaginal candidiasis, topical dextran sulfate administration reduced intravaginal tissue damage and inflammation. Collectively, sulfated GAGs are epithelial cell targets of candidalysin and can be used therapeutically to protect cells from candidalysin-induced damage.

Candida albicans, a commensal fungus, frequently colonizes epithelial surfaces including the skin and the oral, gut and vaginal mucosa. When host defences are dysregulated, *C. albicans* can become pathogenic, causing oropharyngeal, vulvovaginal or haematogenously disseminated candidiasis. A key virulence factor of *C. albicans* is candidalysin, a cytolytic peptide toxin[1–3]. Synthesized as a pro-protein from the *ECE1* gene, the mature 31-amino-acid candidalysin is released from *C. albicans* hyphae[1,4,5], accumulates at high concentrations within the invasion pocket[6–8] and forms pore-like structures on the host cell membranes, causing calcium influx and cell damage[4,7,9,10]. This toxin also stimulates an innate immune response in epithelial cells by activating the epidermal growth factor receptor (EGFR)[3,11], the mitogen-activated protein kinases P38 and extracellular regulated kinases (ERK)1/2 (refs. 12–15), and the c-Fos transcription factor[12,14]. These signalling pathways trigger the production of downstream inflammatory mediators such as IL-6, GM-CSF, CXCL8 and IL-1β, which recruit phagocytes to foci of infection and enhance their fungicidal activities[2,3,11,16,17].

Despite extensive studies on candidalysin[2,4,5,7,8,12], the host determinants that target the binding and oligomerization of this toxin on the host cell surface remain unknown. In this study, we performed a genome-wide loss-of-function clustered regularly interspaced short palindromic repeats (CRISPR) screen in a human oral epithelial cell line to identify specific host factors required for susceptibility to candidalysin-induced cellular damage. We identified the glycosaminoglycan (GAG) biosynthesis genes, *XYLT2*, *B3GALT6* and *B3GAT3*, as crucial for candidalysin susceptibility. The absence of GAGs results

A full list of affiliations appears at the end of the paper. ✉e-mail: sfiller@ucla.edu

in enhanced epithelial cell resistance to damage induced by both candidalysin and live *C. albicans*. Biophysical analyses indicated that candidalysin directly binds to sulfated GAGs, which facilitate its oligomerization or enrichment on the cell surface. Exogenous GAGs or GAG analogues, such as dextran sulfate, bind to candidalysin and inhibit its activity. In a mouse model of vulvovaginal candidiasis, intravaginal administration of dextran sulfate significantly reduces epithelial cell damage, IL-1β release and neutrophil accumulation. Collectively, these data indicate that host GAGs facilitate candidalysin activity and that GAG analogues can be used therapeutically to protect host cells from candidalysin-induced damage.

Results

A CRISPR screen identifies host factors for candidalysin

To identify potential host cell targets of candidalysin, we performed a genome-wide CRISPR–Cas9 knockout screen in the TR146 oral epithelial cell line. Cas9-expressing TR146 cells were transduced with a lentiviral single guide RNA (sgRNA) library (Brunello) that has four sgRNAs for each of 19,114 human genes (Extended Data Fig. 1a,b)[18,19]. The transduced cells were incubated with 30 μM candidalysin for 6 h, which resulted in 60–70% cell death in control TR146 cells, as measured by a 2,3-bis-(2-methoxy-4-nitro-5-sulfophenyl)-2h-tetrazolium-5-carboxanilide (XTT) assay (Extended Data Fig. 1c,d). After five rounds of selection (Fig. 1a), the sgRNA target genes in the surviving cells were identified by sequencing[20]. The fold enrichment of each targeted gene relative to the initial library was ranked by the sigma fold change (FC) score[20] (Fig. 1a).

Mutations that confer host cell resistance to candidalysin

A total of 182 genes were significantly enriched in the screen (Supplementary Table 1). The top seven hits were *B3GALT6*, *TYK2*, *XYLT2*, *B3GAT3*, *SLC39A9*, *GBF1* and *EMP1* (Fig. 1a). To confirm that the products of these genes were required for maximal candidalysin-induced damage, we used CRISPR–Cas9 gene deletion, small interfering RNA (siRNA) knockdown and/or small molecule inhibitors to eliminate or reduce their activities. Each gene knockout or knockdown was confirmed via immunoblot analysis (Extended Data Fig. 2a). Neither the Tyk2 tyrosine kinase nor epithelial cell membrane protein 1 (EMP1) was found to significantly alter epithelial cell susceptibility to candidalysin (Fig. 1b and Extended Data Fig. 2b). Deletion of *SLC39A9*, which is predicted to encode a zinc ion transporter[21], and siRNA knockdown of Gbf1, a Sec7 domain family guanine nucleotide exchange factor protein (Extended Data Fig. 2a)[22], modestly but significantly increased resistance to candidalysin-induced cell damage. Importantly, deletion of *XYLT2*, *B3GALT6* or *B3GAT3* significantly increased host cell resistance to candidalysin (Fig. 1b), increasing the concentration of candidalysin required to cause 50% damage (IC_{50}) by 2.2- to 2.3-fold relative to control cells. *XYLT2*, *B3GALT6* and *B3GAT3* encode enzymes that catalyse the synthesis of the Xyl-Gal-Gal-GlcA tetrasaccharide linker that attaches GAGs to core proteins (Fig. 2a)[23–27]. Deletion of any of the three genes markedly decreased the amount of cell-surface exposed heparan sulfate, as determined by indirect immunofluorescence and flow cytometry (Extended Data Fig. 2c,d). Based on these results, we focused our subsequent experiments on the interactions of GAGs with candidalysin.

Candidalysin binds to GAGs

Next, we investigated whether exogenous GAGs could compete with endogenous cell-surface GAGs for interacting with candidalysin and protect epithelial cells from candidalysin-induced damage. Heparin (a highly sulfated form of heparan sulfate), heparan sulfate and chondroitin sulfate all exhibited dose-dependent protection against candidalysin-induced epithelial cell damage, whereas hyaluronic acid provided no discernible protection (Fig. 2b; see structures in Extended Data Fig. 3a). These results indicate that some, but not all, GAGs can protect oral epithelial cells from damage caused by candidalysin, possibly by competitive binding to candidalysin.

To test this hypothesis, we analysed the kinetics and affinity of the candidalysin–heparin interaction using surface plasmon resonance (SPR). Candidalysin was passed through a sensor chip containing immobilized heparin. The binding kinetics were determined by globally fitting the association and dissociation phases, using a 1:1 Langmuir binding model. The sensorgrams indicated that candidalysin binds to heparin with high affinity at pH 7.4, characterized by a K_D of 32.4 ± 10.2 nM (Fig. 2c). Notably, the dissociation rate constant (k_{off}) of candidalysin from heparin was quite low at $2.30 \pm 0.14 \times 10^{-4}$ s^{-1}, indicating that the half-life of the heparin–candidalysin complex probably exceeds 50 min. Therefore, candidalysin binds to heparin with high affinity and forms a stable complex.

Exogenous sulfated GAGs protect cells from damage

To investigate the specificity of protection from candidalysin-induced damage, we tested additional GAGs and GAG analogues. Hyaluronic acid failed to protect epithelial cells from candidalysin-induced damage, suggesting that protection is not just due to positively charged candidalysin molecules binding to negatively charged GAGs. Also, the highly carboxylated, negatively charged polysaccharide alginate did not ameliorate candidalysin-induced damage, even at the highest concentration tested (128 μg ml^{-1}) (Extended Data Fig. 4a). Thus, the candidalysin interaction with some GAGs cannot be explained by charge–charge interactions alone.

Naturally occurring GAGs differ in the extent and stereochemical positioning of sulfation (Extended Data Fig. 3a). To determine whether sulfation of GAGs is required for their protective effects, we analysed the sulfated and non-sulfated GAG analogues, dextran sulfate and dextran (see structures in Extended Data Fig. 3b). We found that dextran sulfate, but not dextran, protected epithelial cells from candidalysin-induced damage in a dose-dependent manner (Fig. 2d). Dextran sulfate with molecular mass ranging from 10 kDa to 500 kDa was similarly protective, indicating that protection was independent of molecular mass (Extended Data Fig. 4b).

Heparin, heparan sulfate and chondroitin sulfate are negatively charged linear polysaccharides[28–30], whereas dextran sulfate has a branched structure. Yet, all these molecules protected cells against candidalysin-induced damage. This result suggested that the protective effects of GAGs and GAG analogues may be largely independent

Fig. 1 | Genes identified by the genome-wide CRISPR screen that are required for maximal candidalysin-induced epithelial cell damage. a, Schematic diagram of the genome-wide CRISPR screen used to identify genes required for susceptibility to candidalysin-induced epithelial cell damage and scatter plot of the results. The shape of the symbols indicates the number of sgRNAs targeting each gene that were significantly enriched in the screen. The sigma FC gene rank for each gene was calculated by adding the fold changes of all sgRNAs that target that gene, multiplied by the number of sgRNAs that showed significant enrichment. The top seven enriched genes (sigma FC > 6) are labelled in the plot. *P* values were calculated using the adjusted robust rank aggregation (α-RRA) and STARS, a gene-ranking algorithm for genetic perturbation screens, and adjusted for multiple hypothesis tests using the Benjamini–Hochberg FDR procedure. **b**, Effects of CRISPR deletion (*B3GAT3*, *XYLT2*, *B3GALT6*, *SLC39A9*, *EMP1*), pharmacologic inhibition (Tyk2) and siRNA knockdown (*GBF1*) on the survival of oral epithelial cells after 6 h of candidalysin exposure. The left panels show the survival (measured by an XTT assay) of epithelial cells exposed to the indicated concentrations of candidalysin. The plots represent the combined results of three to four experiments, each performed in triplicate. The right panels show the concentration of candidalysin that yielded 50% survival (IC_{50}), which was calculated from the data in the corresponding graph in the left panels. Results are mean ± s.d. *P* values were calculated using the unpaired, two-sided Student's *t*-test. Credit: **a**(top), Servier Medical Art under a Creative Commons license CC BY 4.0.

https://doi.org/10.1038/s41564-024-01794-8

of the structure of the backbone molecule. In support of this hypothesis, sulfated α-cyclodextrin (a cyclic hexasaccharide; see structure in Extended Data Fig. 3b) was also protective, but only when it was sulfated (Fig. 2d). These sulfated GAGs and their analogues were also protective against 70 μM candidalysin, a highly lethal concentration, although the extent of protection was decreased (Extended Data Fig. 4c). The protective effects of dextran sulfate lasted at least 24 h (Extended Data Fig. 4d). These data suggest that sulfation of GAG or its analogues is

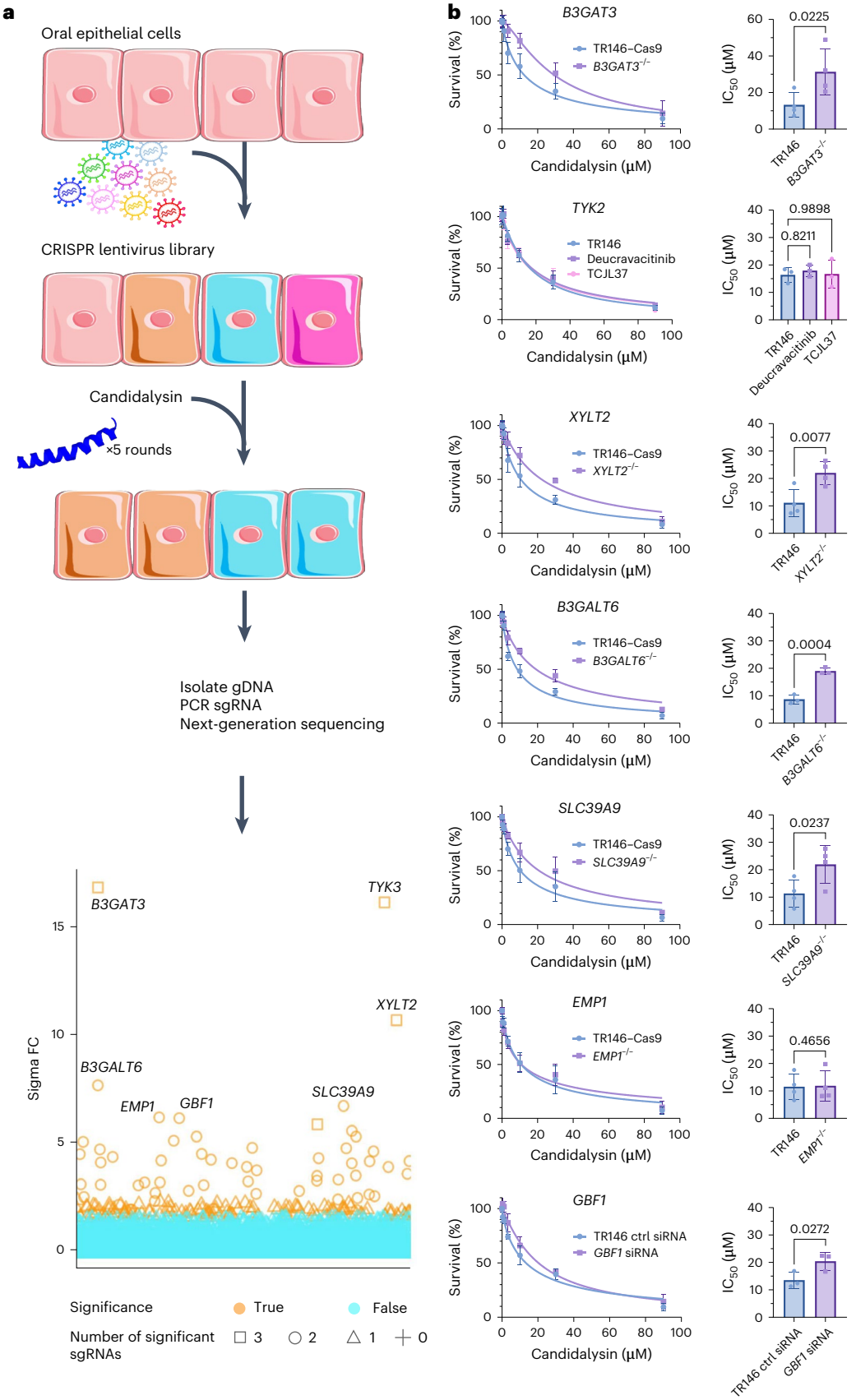

https://doi.org/10.1038/s41564-024-01794-8

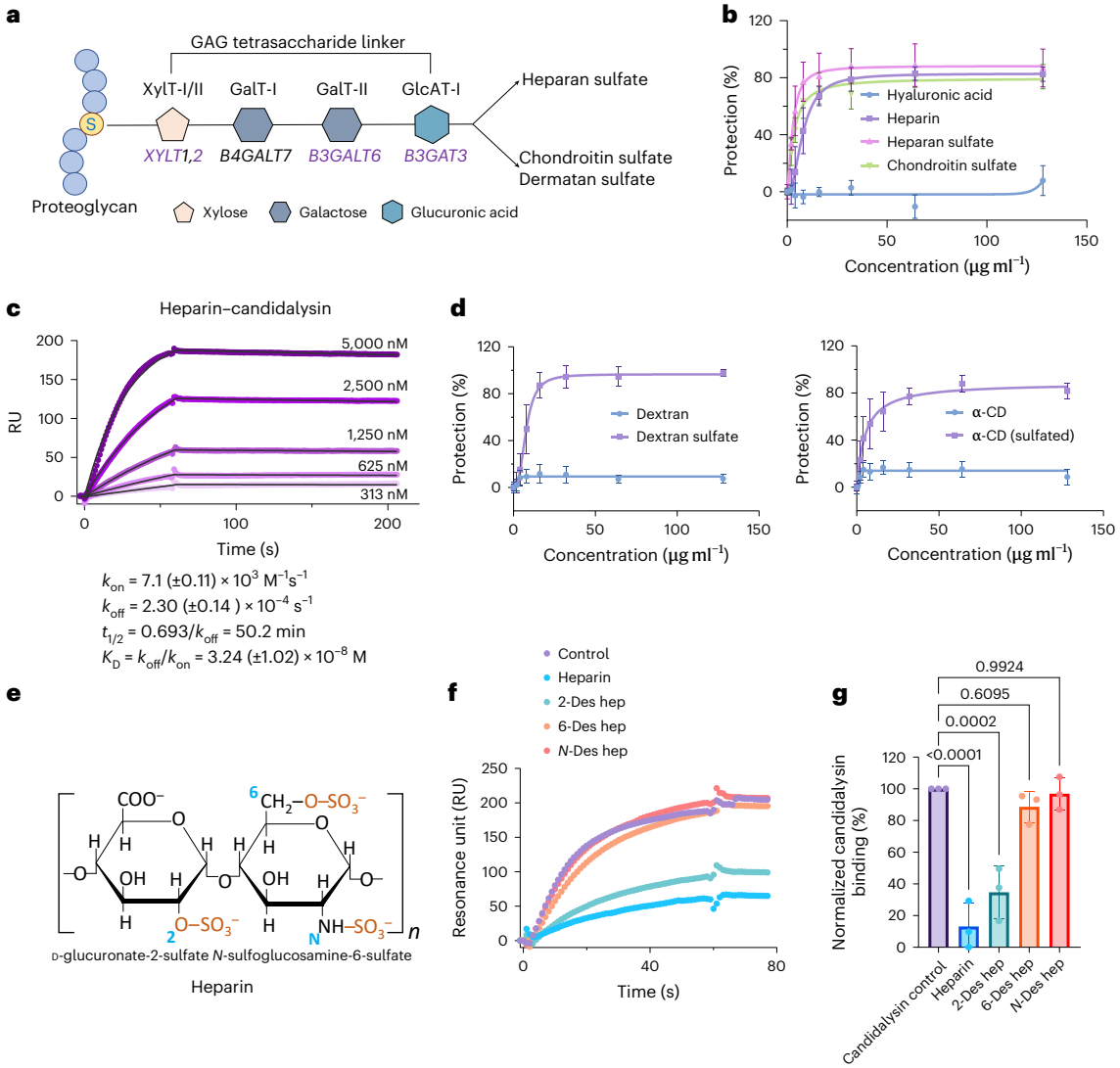

Fig. 2 | Sulfated GAGs and dextrin analogues bind to candidalysin and provide dose-dependent protection to epithelial cells against candidalysin-induced damage. a, Diagram illustrating the enzymes that catalyse the biosynthesis of the tetrasaccharide linker present in all GAGs. The genes that encode the enzymes are denoted under the monosaccharide, and the ones in purple are those identified by the CRISPR screen. **b**, Protection from damage caused by a 6 h exposure to 30 μM candidalysin provided by the indicated GAGs as measured by an XTT assay. The curves were generated from the data of three independent experiments, each performed in triplicate. Percentage protection was calculated as the normalized increase in host cell survival relative to control cells treated with candidalysin alone. **c**, SPR sensorgram of the interaction of candidalysin with heparin immobilized on the biosensor chip. The concentration of candidalysin used to generate each sensorgram is indicated on the graph. The binding kinetics (k_{on}, association rate constant; k_{off}, dissociation rate constant; $t_{1/2}$, half-life; and $K_D = k_{on}/k_{off}$, binding equilibrium dissociation constant) were calculated from the global fitting of the five concentrations using a 1:1 Langmuir binding model. **d**, Protection from damage caused by a 6 h exposure to 30 μM candidalysin provided by dextran, dextran sulfate, α-cyclodextrin (α-CD) or sulfated α-cyclodextrin measured by an XTT assay. The curves were generated from the data of three independent experiments. **e**, Structure of heparin showing the location of the sulfate groups. **f**, Representative surface plasmon resonance sensorgrams showing the effects of 2-*O*-desulfated heparin (2-Des hep), 6-*O*-desulfated heparin (6-Des hep) and *N*-desulfated heparin (*N*-Des hep) on the interaction of candidalysin with heparin on the biosensor chip. **g**, Combined results of three independent experiments showing the inhibitory effects of the various desulfated heparins on the interaction of candidalysin with heparin. Results are mean ± s.d. *P* values were calculated using one-way ANOVA with Dunnett's multiple-comparison test.

critical for protection from candidalysin-induced cell damage, whereas the molecular mass or the structure of the backbone molecule is less important.

To determine whether the location of the sulfate moiety on the backbone molecule affects binding to candidalysin, we used SPR to test the capacity of various desulfated heparins to compete with native heparin for binding to candidalysin. While preincubation of candidalysin with heparin and 2-*O*-desulfated heparin inhibited candidalysin binding to chip-immobilized heparin, *N*-desulfated heparin and 6-*O*-desulfated heparin failed to inhibit this binding (Fig. 2e–g). Thus, both the *N*-sulfo and 6-*O*-sulfo groups on heparin are required for candidalysin binding, underscoring the importance of stereospecific sulfate modifications of GAGs.

Using an SPR-based competition assay, we assessed the capacity of various GAGs to inhibit the interaction between candidalysin and chip-immobilized heparin. Dextran, chondroitin sulfate A (chondroitin-4-sulfate), chondroitin sulfate B (dermatan sulfate), chondroitin sulfate C (chondroitin-6-sulfate) and heparan sulfate did not significantly inhibit candidalysin binding to chip-immobilized heparin (Extended Data Fig. 4e,f). By contrast, heparin and dextran sulfate both inhibited binding, with dextran sulfate reducing binding by >95% (Extended Data Fig. 4e,f). These results suggest that dextran

https://doi.org/10.1038/s41564-024-01794-8

sulfate has the highest binding affinity for candidalysin, followed by heparin and then the other GAGs that were tested.

GAGs facilitate polymerization and aggregation of candidalysin

It has been previously shown that candidalysin forms linear and circular structures (loops) in aqueous solution before inserting into the cell membrane to form pores[4]. Using transmission electron microscopy, we verified that candidalysin formed these structures when added to a solid substrate in the presence of dextran or the vehicle control (Extended Data Fig. 5a). The loops, which probably become pores when inserted into a membrane, were replaced by aggregates in the presence of dextran sulfate or heparan sulfate. Atomic force microscopy (AFM) confirmed that free dextran sulfate and heparan sulfate, but

Fig. 3 | GAGs enhance candidalysin polymerization and aggregation. **a**, Atomic force microscopic images of supported DOPC lipid bilayers exposed to 333 nM candidalysin with or without 5 μg ml^{-1} dextran, dextran sulfate and heparan sulfate (upper panel), and quantification of the number of pores per μm^2 for each treatment (lower panel). Scale bars: 200 nm. Results are the mean ± s.d. of three experiments. **b**, Effects of incubating candidalysin in 1 μM C-laurdan for 4 h on the GP score (left panel). The effects of dextran sulfate on the GP scores of 0.2 μM and 0.5 μM candidalysin (right panel). Results are the mean ± s.d. of three independent experiments. **c**,**d**, Colocalization of candidalysin with heparan sulfate on the surface of wild-type TR146 (**c**) or GAG-deficient *B3GAT3*$^{-/-}$ (**d**) epithelial cells incubated with CFSE-labelled candidalysin (10 μM) for the indicated times. The arrows indicate representative candidalysin aggregates. Scale bars: 20 μm. The scale bar in **c** and **d** applies to all images in each panel. **e**, Quantification of the number of candidalysin aggregates per microscopic field on the indicated cells after 20 min of exposure to CFSE–candidalysin. Results are the mean ± s.d. of three random microscopic fields per experiment from three independent experiments. **f**, Interaction of CFSE–candidalysin with a 1:1 mixture of TR146 and GAG-deficient *B3GAT3*$^{-/-}$ cells for 20 min. The arrows indicate representative candidalysin aggregates. The TR146 cells stain for heparan sulfate (red) and are marked with asterisks. Scale bar: 20 μm. The scale bar in **f** applies to all images in the panel. **g**, Quantification of the candidalysin aggregates per TR146 or *B3GAT3*$^{-/-}$ cell in the mixed population of TR146 and *B3GAT3*$^{-/-}$ cells. Results are the mean ± s.d. of five random fields per experiment from three independent experiments. **h**, Effects of calcium ionophore A23187 (1 μM) or candidalysin (10 μM) on the levels of free intracellular calcium in TR146 and *B3GAT3*$^{-/-}$ cells as determined by flow cytometry. The period 0–90 s represents the baseline levels, and data collection was resumed at 120 s after treatment. Results are the mean ± s.d. of four independent experiments. *P* values were calculated using one-way ANOVA with Dunnett's multiple-comparison test (**a**,**b**) and the unpaired, two-sided Student's *t*-test (**e**,**g**).

not dextran, caused candidalysin to form aggregates, which appeared as bright white structures (Extended Data Fig. 5a). AFM imaging of candidalysin on a 1,2-dioleoyl-sn-glycero-3-phosphocholine (DOPC) bilayer showed that candidalysin formed pores on the bilayer either alone or in the presence of dextran (Fig. 3a), but not in the presence of heparan sulfate or dextran sulfate. Collectively, these data suggest that binding to free sulfated GAGs leads to polymerization (aggregation) of candidalysin. This interaction with sulfated GAGs on the cell surface probably increases the concentration of the peptide on the cell membrane, promoting its pore-forming ability. By contrast, the aggregates observed in the presence of exogenous GAGs are probably non-functional, because they reduce the number of pore-competent loops.

To test this hypothesis, we measured the response of 6-dodecanoyl-2-[*N*-methyl-*N*-(carboxymethyl)amino]naphthalene (C-laurdan) to candidalysin. When C-laurdan is dissolved in a polar solvent, its emission spectrum shifts by approximately 50 nm (refs. 31,32). We analysed the concentration-dependent effects of candidalysin on the fluorescence emission of C-laurdan to calculate a generalized polarization (GP) score, which increases as binding to or polymerization and aggregation of candidalysin reduce the local hydration of the dye (Extended Data Fig. 5b). The GP score rose as the concentration of candidalysin increased owing to increased peptide polymerization (Fig. 3b). Incubation of candidalysin with dextran sulfate further increased the GP score, indicating greater candidalysin polymerization and/or aggregation (Fig. 3b). In the absence of candidalysin, dextran sulfate had no effect on the GP score (Extended Data Fig. 5c). We also found that candidalysin caused membrane permeation when added to artificial vesicles composed of DOPC or 1-palmitoyl-2-oleoyl-sn-glycero-3-phosphocholine (POPC), which was delayed when dextran sulfate was added before candidalysin (Extended Data Fig. 5d). Thus, dextran sulfate enhances the self-assembly of candidalysin in an aqueous solution and delays pore formation.

Next, we used confocal microscopic imaging of epithelial cells that were incubated with carboxyfluorescein succinimidyl ester (CFSE)-labelled candidalysin to investigate how cell surface GAGs alter the interactions of candidalysin with these cells. The CFSE–candidalysin remained functional, damaging epithelial cells similarly to unlabelled candidalysin (Extended Data Fig. 5e). When added to wild-type TR146 cells, the CFSE–candidalysin formed aggregates that increased in number and size over time (Fig. 3c). These aggregates colocalized with heparan sulfate (Extended Data Fig. 5f), suggesting that candidalysin interacts with cell surface GAGs. Candidalysin also caused a progressive loss of surface exposed heparan sulfate, so that by 30 min very little heparan sulfate could be detected. These results indicate that candidalysin interacts with GAGs on the epithelial cell surface.

When CFSE–candidalysin was added to GAG-deficient *B3GAT3*$^{-/-}$ cells (Extended Data Fig. 2c,d), which are more resistant to candidalysin damage relative to TR146 cells (Fig. 1b), we observed that candidalysin aggregates were less numerous and more diffuse (Fig. 3c–e). In a mixed population of wild-type TR146 and GAG-deficient *B3GAT3*$^{-/-}$ cells, candidalysin preferentially localized to the GAG-sufficient wild-type cells (Fig. 3f,g). This preferential binding to GAG-expressing cells probably protected the GAG-deficient cells from candidalysin-induced damage, providing an explanation for why genes required for GAG biosynthesis were among the top hits in our CRISPR screen. These data further support the idea that sulfated GAGs bind to candidalysin and facilitate its polymerization on the cell surface.

The polymerization of candidalysin results in the formation of pores in the plasma membrane, leading to an influx of calcium into the cell[1]. To determine whether the observed reduction in candidalysin aggregates in the *B3GAT3*$^{-/-}$ cells resulted in decreased pore formation, we used flow cytometry to measure the influx of calcium in epithelial cells after treatment with candidalysin. We found that candidalysin induced a much smaller increase in intracellular calcium in the GAG-deficient *B3GAT3*$^{-/-}$ cells compared with wild-type TR146 cells (Fig. 3h). By contrast, the kinetics of intracellular calcium increase into these cells were similar when they were incubated with the A23187 calcium ionophore. Thus, the formation of functional candidalysin pores occurs more slowly in the absence of cell surface GAGs.

GAGs mediate epithelial cell responses to live *C. albicans*

To test whether sulfated GAGs are required for the pathogenic interactions of *C. albicans* with oral epithelial cells, we analysed the interactions

Fig. 4 | Sulfated GAGs mediate epithelial cell invasion, damage and stimulation of oral epithelial cells by live *C. albicans*. **a**,**b**, *C. albicans* association with (**a**) and endocytosis by (**b**) wild-type and *B3GAT3*$^{-/-}$, *XYLT2*$^{-/-}$ and *B3GALT6*$^{-/-}$ mutant epithelial cells. The average numbers of organisms per high-power field (HPF) that were associated with and endocytosed by TR146 cells were 12.84 ± 4.97 and 2.91 ± 1.27, respectively. Results are the mean ± s.d. of four experiments, each performed in triplicate. **c**, Protection against damage caused by 5 h of infection with live, wild-type *C. albicans* at an MOI of 5 in *B3GAT3*$^{-/-}$, *XYLT2*$^{-/-}$ and *B3GALT6*$^{-/-}$ mutant cells relative to wild-type TR146 epithelial cells, as measured by an XTT assay. Results are the mean ± s.d. of three experiments, each performed in replicates of four. **d**, Effects of dextran and dextran sulfate (100 μg ml^{-1}) on damage to TR146 and *B3GAT3*$^{-/-}$ cells caused by 5 h of infection with live *C. albicans* SC5314 at an MOI of 5, as measured by an LDH release assay. Results are the mean ± s.d. of five experiments, each performed in triplicate. **e**,**f**, Effects of dextran and dextran sulfate (100 μg ml^{-1}) on wild-type *C. albicans* association with (**e**) and endocytosis by (**f**) the indicated epithelial cells. The average numbers of organisms per high-power field that were associated with and endocytosed by TR146 cells were 9.64 ± 2.68 and 1.88 ± 0.56, respectively. Results are the mean ± s.d. of four experiments, each performed in triplicate. *P* values were calculated using unpaired, two-tailed Student's *t*-test (**a**–**c**) or one-way ANOVA with Dunnett's multiple-comparison test (**d**–**f**). DX, dextran; DS, dextran sulfate.

https://doi.org/10.1038/s41564-024-01794-8

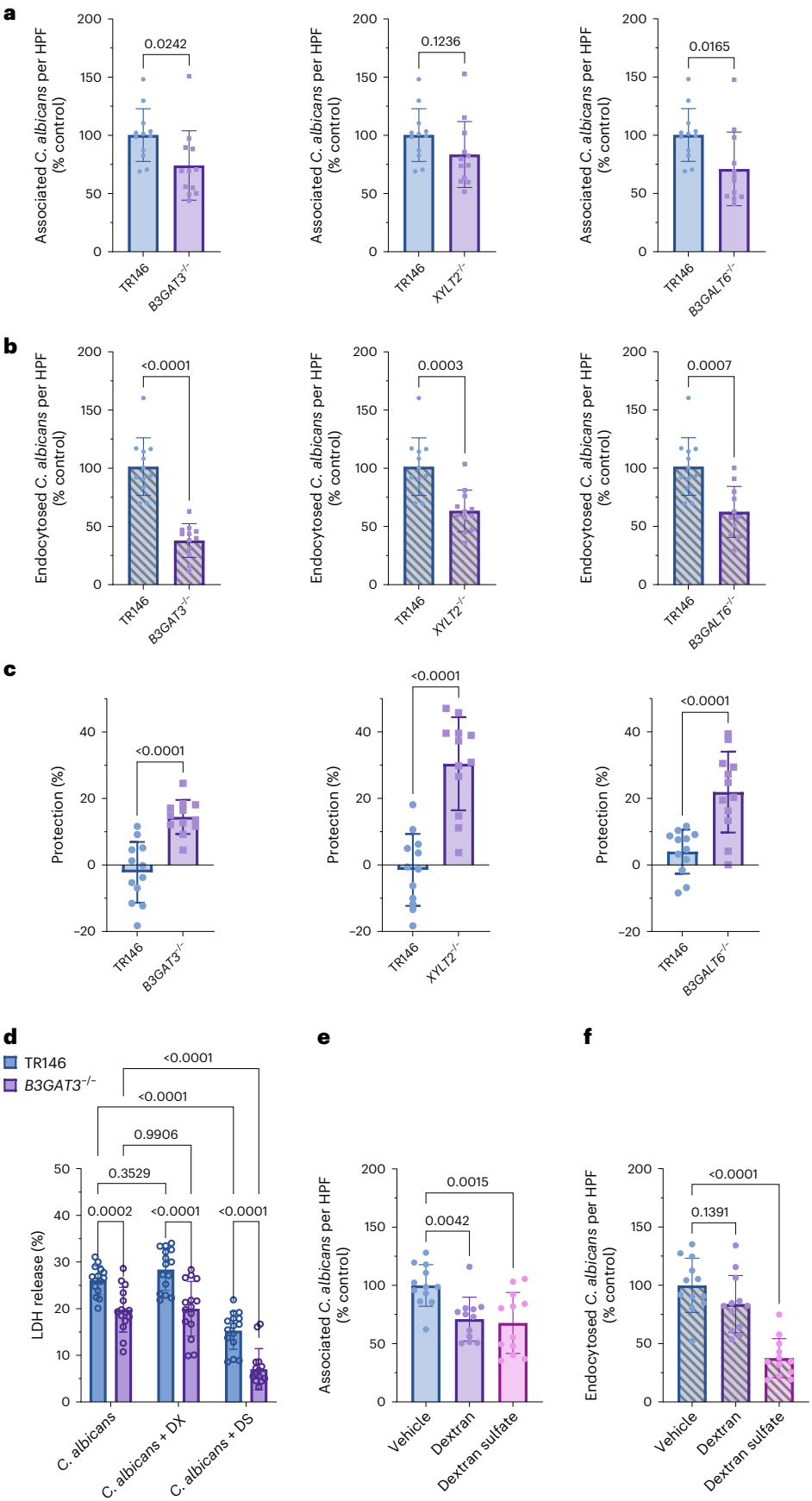

https://doi.org/10.1038/s41564-024-01794-8

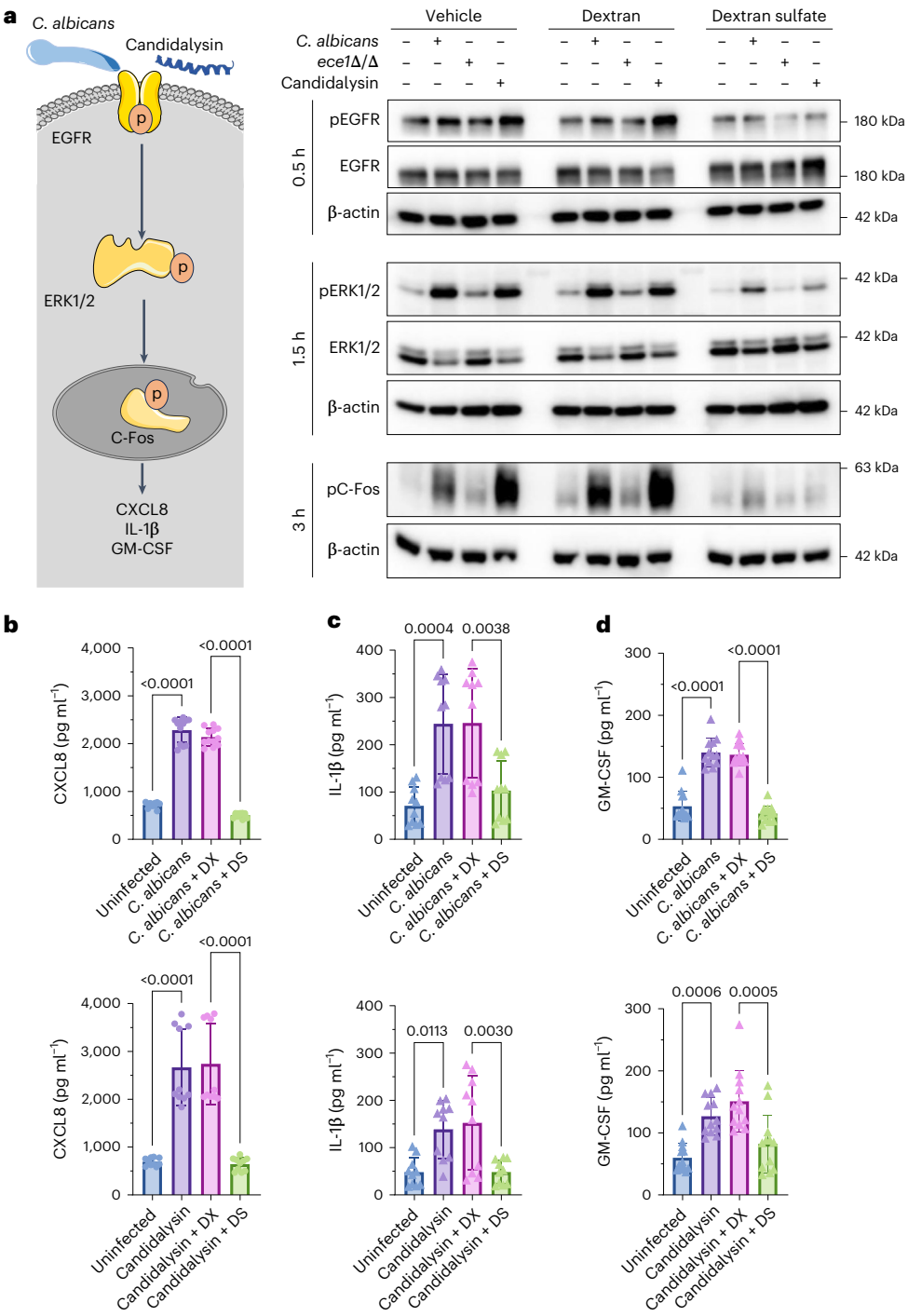

Fig. 5 | Sulfated GAGs mediate stimulation of oral epithelial cells by candidalysin and live *C. albicans*. **a**, Simplified model of epithelial immune signalling in response to *C. albicans* and candidalysin (left panel). Immunoblot analysis of the effects of dextran (100 μg ml^{-1}) and dextran sulfate (100 μg ml^{-1}) on the phosphorylation of EGFR, ERK1/2 and the C-Fos transcription factor in TR146 cells induced by wild-type *C. albicans* SC5314 or the *ece1*Δ/Δ mutant at an MOI of 5, or candidalysin (10 μM) at the indicated time points (right panel). Shown are the representative results of three independent experiments. **b**–**d**, Effects of dextran and dextran sulfate (100 μg ml^{-1}) on the production of CXCL8 (**b**), IL-1β (**c**) and GM-CSF (**d**) by TR146 cells infected with *C. albicans* SC5314 (MOI = 5, top) or incubated with candidalysin (10 μM, bottom) for 6 h. Results in **b**–**d** are the mean ± s.d. of three experiments, each performed in triplicate or replicates of four. *P* values were calculated using one-way ANOVA with Dunnett's multiple-comparison test (**b**–**d**). Credit: **a**(left), Servier Medical Art under a Creative Commons license CC BY 4.0.

of live *C. albicans* with wild-type TR146 cells, and the GAG-deficient *B3GAT3*$^{-/-}$, *B3GALT6*$^{-/-}$ and *XYLT2*$^{-/-}$ cells. Although live *C. albicans* cells had slightly reduced cell association (a measure of adherence) to the GAG-deficient cells, their endocytosis by and damage to these cells were substantially decreased (Fig. 4a–c). Thus, epithelial cell GAGs are required for maximal *C. albicans* adherence, invasion and damage in vitro.

We also tested the effects of dextran sulfate on epithelial cell damage caused by live *C. albicans*. To facilitate comparison with previous studies[1,3,33,34], we measured the extent of epithelial cell damage using a

lactate dehydrogenase (LDH) release assay. This assay yielded similar results to the XTT assay (Fig. 4a,c). We found that dextran sulfate partially protected wild-type TR146 cells from damage caused by wild-type *C. albicans* SC5314, whereas dextran had no effect (Fig. 4d). Although *C. albicans* caused less damage to *B3GAT3*$^{-/-}$ cells than to wild-type TR146 cells, dextran sulfate caused a further reduction in damage (Fig. 4d). Because the candidalysin-deficient *ece1*Δ/Δ mutant did not cause detectable damage to TR146 or *B3GAT3*$^{-/-}$ cells (Extended Data Fig. 5g), we were unable to determine the effects of dextran sulfate on epithelial cell damage caused by this strain. These data indicate that dextran sulfate reduces *C. albicans*-induced epithelial cell damage by both GAG-dependent and GAG-independent mechanisms.

Next, we assessed the effects of dextran and dextran sulfate on *C. albicans* adherence to and endocytosis by oral epithelial cells, testing both the wild-type and *ece1*Δ/Δ mutant strains. Both dextran and dextran sulfate caused a modest, yet statistically significant, reduction in the adherence of wild-type *C. albicans* to oral epithelial cells (Fig. 4e). Both compounds trended towards reducing adherence of the *ece1*Δ/Δ mutant, but this decrease was not significant (Extended Data Fig. 5h). Dextran sulfate decreased the endocytosis of the wild-type strain and the *ece1*Δ/Δ mutant by approximately 60% (Fig. 4f and Extended Data Fig. 5i). Thus, dextran sulfate decreases not only the extent of *C. albicans*-induced damage to oral epithelial cells, but also the capacity of the organism to adhere to and invade these cells. As candidalysin does not mediate adherence to or invasion of oral epithelial cells, the inhibitory effects of dextran sulfate on these processes is independent of its effects on candidalysin.

Infection of epithelial cells with some strains of *C. albicans*, such as SC5314, induces a robust pro-inflammatory response, and candidalysin is one of the main inducers of this response[3,12]. Exposure of oral epithelial cells to live C. *albicans* or candidalysin triggers the phosphorylation of the EGFR[35], ERK1/2 signalling cascade and, consequently, phosphorylation of the c-Fos transcription factor[12,14], a result we confirmed (Fig. 5a). Dextran sulfate, but not dextran, inhibited the phosphorylation of EGFR, ERK1/2 and c-Fos induced by either wild-type *C. albicans* or candidalysin in both wild-type TR146 and *B3GAT3*$^{-/-}$ oral epithelial cells (Fig. 5a and Extended Data Fig. 6a). As expected, the *ece1*Δ/Δ mutant did not stimulate phosphorylation of EGFR, ERK1/2 and c-Fos above basal levels in either epithelial cell line. These results indicate that while GAGs are not required for *C. albicans* or candidalysin to stimulate oral epithelial cells, dextran sulfate can inhibit their response to both stimuli.

Activation of oral epithelial cells by either live *C. albicans* or candidalysin induces these cells to secrete cytokines such as CXCL8, IL-1β and GM-CSF (Fig. 5b–d). Dextran sulfate, but not dextran, significantly decreased the production of these cytokines in wild-type TR146 cells. (Fig. 5b–d). While exposure of *B3GAT3*$^{-/-}$ epithelial cells to *C. albicans* stimulated the production of these cytokines, candidalysin induced only the secretion of CXCL8 and GM-CSF but not IL-1β (Extended Data Fig. 6b). These responses were almost completely inhibited by dextran sulfate, but not dextran. The *ece1*Δ/Δ mutant did not induce a detectable increase in secretion of any of these cytokines by either *B3GAT3*$^{-/-}$ or wild-type TR146 cells (Extended Data Fig. 6b,c). Thus, dextran sulfate interferes with the signalling cascade that induces the production of pro-inflammatory mediators in response to *C. albicans* and candidalysin.

Dextran sulfate ameliorates vulvovaginal candidiasis

To evaluate whether dextran sulfate could interfere with *C. albicans* pathogenicity in vivo, we tested it in a mouse model of mucosal candidiasis. We could not test the effects of dextran sulfate in the mouse model of oropharyngeal candidiasis because the compound would need to be administered continuously to prevent it from being cleared from the oropharynx by salivary flow. To circumvent this problem, we analysed the efficacy of dextran sulfate in a mouse model of vulvovaginal candidiasis, where it remained in the vagina for an extended time. Before conducting this study, we verified that dextran sulfate could protect the A431 vulval epithelial cell line from candidalysin-induced damage (Fig. 6a). Dextran sulfate also diminished the production of IL-1β and CXCL8 by these cells induced by either live *C. albicans* or candidalysin (Fig. 6b).

In the mouse model of vulvovaginal candidiasis, daily administration of dextran sulfate intravaginally significantly decreased the extent of host cell damage in the vagina (Fig. 6c). Dextran sulfate also reduced vaginal inflammation, as reflected by reduced levels of neutrophils and IL-1β (Fig. 6d,e). By contrast, this treatment did not significantly alter the vaginal fungal burden (Fig. 6f). Histopathologic analyses verified that the dextran-sulfate-treated mice exhibited less damage to the vaginal epithelium and lower neutrophil accumulation compared with mice treated with vehicle alone (Fig. 6g). We also tested the effects of dextran sulfate on the outcome of vaginal candidiasis in CD-1 mice, which are reported to be resistant to this infection[35]. In the mice that achieved a high vaginal fungal burden, dextran sulfate treatment significantly reduced tissue damage and decreased neutrophil accumulation (Extended Data Fig. 7a,b). While there was a trend towards reduced IL-1β in the dextran-sulfate-treated mice, this difference was not statistically significant (Extended Data Fig. 7c). As was found in C57BL/6 mice, dextran sulfate treatment had no effect on the vaginal fungal burden (Extended Data Fig. 7d). Thus, dextran sulfate ameliorates vaginal candidiasis in two different mouse strains.

Discussion

Through a genome-wide CRISPR knockout screen, we identified three genes, *B3GAT3*, *B3GALT6* and *XYLT2*, that are required for maximal susceptibility to candidalysin-induced host cell damage. The products of each of these genes catalyse linear, early steps in GAG biosynthesis in

Fig. 6 | Dextran sulfate protects vaginal epithelial cells from damage and inhibits pro-inflammatory cytokine production in vitro and during mouse vulvovaginal candidiasis. a, Survival of A431 vulvar epithelial cells after incubation with 30 μM candidalysin for 6 h (left). Protection from candidalysin-induced damage by dextran and dextran sulfate (right). Results are the mean ± s.d. of three to four experiments, each performed in triplicate. **b**, Effects of dextran and dextran sulfate (100 μg ml^{-1}) on the production of IL-1β and CXCL8 by vulval epithelial cells incubated with *C. albicans* (MOI = 5) or candidalysin (10 μM) for 24 h. Results are the mean ± s.d. of three experiments, each performed in duplicate or triplicate. **c**–**f**, C57BL/6 mice were administered either dextran sulfate or vehicle alone intravaginally before inoculation with *C. albicans* and once daily thereafter. After 3 days of infection, the concentrations of adenylate kinase (RLU, relative light units) (a measure of host cell damage) (**c**), neutrophils (PMN) (**d**), IL-1β (**e**) and fungal colony forming units (CFU) (**f**) in the vaginal lavage fluid were determined. Results in **c**–**f** are the mean ± s.d. of two experiments, one that used three mice per condition and another that used four mice per condition. **g**, Representative images of haematoxylin and eosin (H&E)-stained histological sections of vaginal tissue on day 3 post-infection. The scale bars represent 200 μm in full images and 50 μm in magnified images. **h**, A proposed working model of how cell surface GAGs facilitate *C. albicans* and candidalysin-induced cell damage and the protective effects of exogenous dextran sulfate. Free candidalysin binds to cell surface GAGs such as heparan sulfate or chondroitin sulfate (1). Binding to cell surface GAGs enhances the aggregation and polymerization of candidalysin (2), which facilitates pore formation on the host cell plasma membrane (3), leading to host cell damage. Exogenous dextran sulfate causes aggregation of candidalysin extracellularly. *C. albicans* cells adhere to and invade epithelial cells to cause cell damage. Exogenous dextran sulfate binds to *C. albicans*, reducing adherence to and invasion of host cells. *P* values were calculated using unpaired, two-sided Student's *t*-test (**a**,**c**–**f**) or one-way ANOVA with Dunnett's multiple-comparison test (**b**). Credit: **h**, Servier Medical Art under a Creative Commons license CC BY 4.0.

https://doi.org/10.1038/s41564-024-01794-8

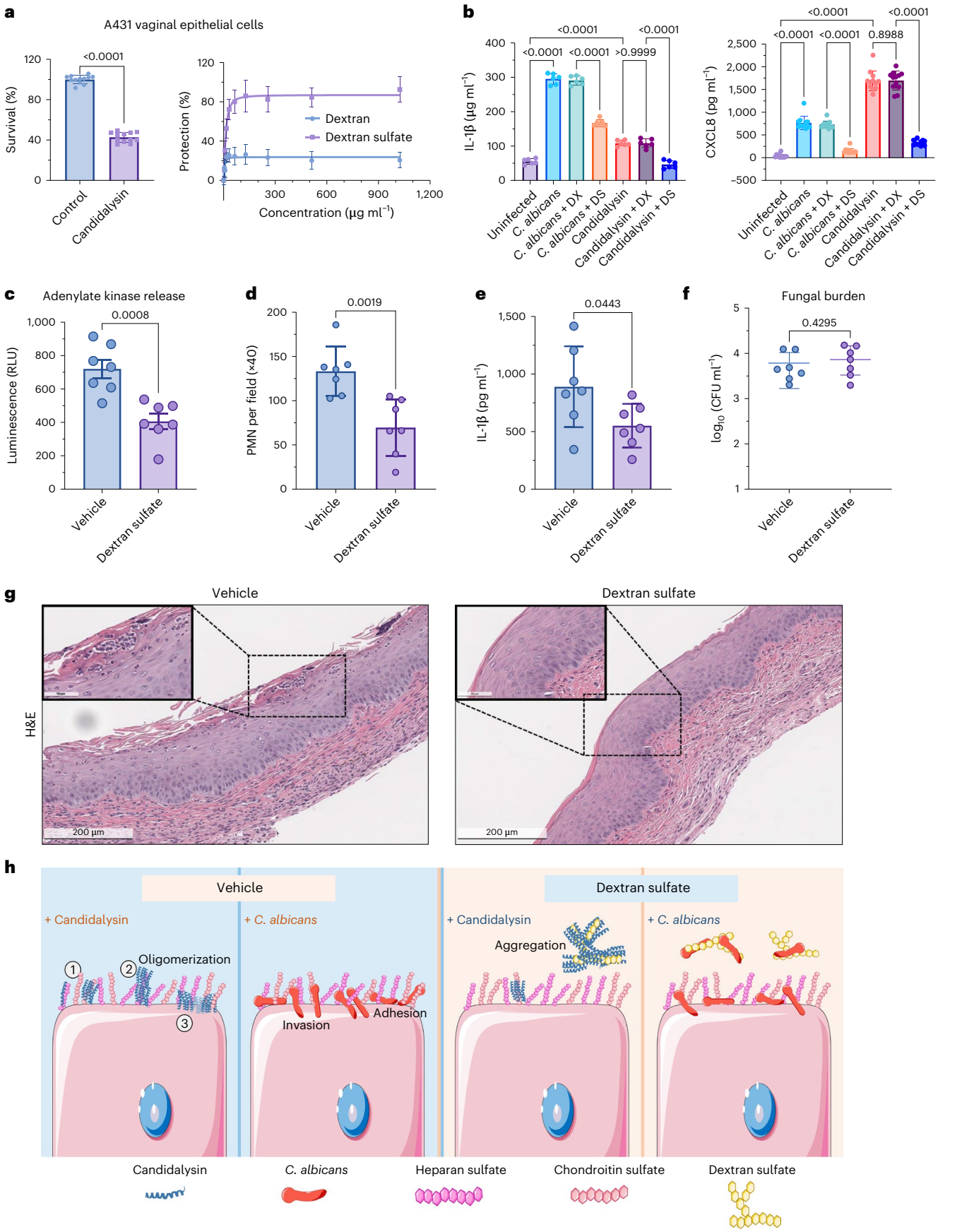

host cells. We subsequently found that candidalysin binds to sulfated GAGs and that the GAG analogue dextran sulfate ameliorates epithelial cell damage and reduces cytokine release induced by both candidalysin and live *C. albicans*. Dextran sulfate was protective both in vitro and in the mouse model of vulvovaginal candidiasis. Collectively, our data indicate that GAGs play a key role in the interactions of candidalysin and *C. albicans* with host epithelial cells.

Glycans have been found to be critical host receptors for bacterial and viral virulence factors[21,36–40]. Nevertheless, their role as targets of fungal virulence factors is poorly understood. Although previous studies indicated that candidalysin interacts with cell membranes[4,10], the current work shows that the interaction of candidalysin with cell surface GAGs is required for the full activity of this toxin. Thus, the work presented here shows the importance of host glycans in the pathogenesis of fungal infections.

B3GAT3, *B3GALT6* and *XYLT2*, which we found were required for maximal candidalysin-induced damage, are among the top hits in numerous other CRISPR screens aimed at identifying key host factors for viral and bacterial pathogenicity[36,37,39–42]. Unlike other screens, our study did not identify *EXT1*, *EXT2* and *EXT3*, which encode glycosyltransferases that are crucial for linear chain extension during the synthesis of heparan sulfate[36,37,43]. While these enzymes are required only for the biosynthesis of heparan sulfate, B3gat3, B3galt6 and Xylt2 are essential for the biosynthesis of all naturally occurring sulfated GAGs, including heparan sulfate, chondroitin sulfate and dermatan sulfate. Thus, our results indicate that candidalysin interacts with most sulfated GAGs to enhance host cell damage. In support of this conclusion, we showed that exogenous heparin, heparan sulfate and chondroitin sulfate could protect epithelial cells against candidalysin-induced damage in a competition assay.

Our screen also identified *SLC39A9* as a gene required for maximal candidalysin-induced damage. This gene was previously identified in a CRISPR screen for resistance to the subtilase cytotoxin SubAB[21]. Interestingly, deletion of *SLC39A9* was shown to reduce N- and O-glycan modification of cell surface proteins[21]. Thus, it is possible that SLC39A9 is required for the surface expression of GAGs that bind to candidalysin.

Recently, the intracellular host cell ligands of various Ece1 peptides, including candidalysin, were identified using a yeast two-hybrid screen[44]. It was found that candidalysin binds to CCNH, a regulatory subunit of the CDK-activating kinase complex. This binding inhibits DNA repair, both in vitro and in the mouse model of oropharyngeal candidiasis. As expected, the yeast two-hybrid screen did not identify B3gat3, B3galt6 or Xylt2 because our data indicate that candidalysin binds to GAGs, which are the products of these enzymes, and not the enzymes themselves.

Using AFM and transmission electron microscopy (TEM), we found that GAGs facilitate candidalysin polymerization or aggregation. Our immunofluorescence and flow cytometry assays further confirmed that candidalysin interacts with GAGs on the epithelial cell surface, and GAG-deficient cells show less efficient candidalysin attachment, aggregation and pore formation. These data strongly support our hypothesis that sulfated GAGs provide a platform for candidalysin to oligomerize on the cell surface and enhance the cytotoxic activity of candidalysin.

Exogenous sulfated GAGs and dextran sulfate almost completely blocked epithelial cell damage by competitive binding to candidalysin. However, the GAG-deficient *B3GAT3*$^{-/-}$, *B3GALT6*$^{-/-}$ and *XYLT2*$^{-/-}$ epithelial cells were only partially resistant to candidalysin-induced damage. This result is concordant with previous findings[4] and our own data, which show that candidalysin can induce membrane damage in GAG-free liposomes composed of the synthetic lipids POPC or DOPC. Thus, our results indicate that while GAGs enhance the polymerization of candidalysin at or near the cell surface, this process can occur in the absence of cell surface GAGs, albeit less efficiently.

Candidalysin shows a net positive charge at physiological pH owing to the three lysine residues in its C-terminus[1,45]. Several publications have shown that the cytotoxicity of candidalysin can be mitigated by negatively charged molecules such as albumin, heparin and polyacrylic acid[45–47]. By contrast, we found that the negatively charged hyaluronic acid and alginitic acid failed to protect cells from candidalysin-induced damage. These seemingly divergent results may have occurred because the concentrations of hyaluronic acid and alginitic acid used in our experiments were 1- to 2-log lower than the concentrations of albumin and polyacrylic acid used in the other studies. Notably, our surface plasmon resonance assays revealed a strong binding affinity between candidalysin and heparin ($K_D = 3.24 \times 10^{-8}$ M), highlighting the specificity and strength of this interaction. Furthermore, the importance of *N*- and 6-*O*-sulfate groups on heparin for the heparin–candidalysin interaction implies that charge density and/or stereospecific sulfation patterns, rather than electrostatics, structural attributes or molecular weight alone, determine the interaction strength of GAGs with candidalysin.

We also found that cell surface GAGs are required for maximal *C. albicans* adherence to and invasion of oral epithelial cells. Deletion of *B3GAT3*, *B3GALT6* or *XYLT2* modestly reduced adherence and substantially reduced invasion of *C. albicans* into these cells. Dextran sulfate also inhibited epithelial cell invasion in a candidalysin-independent manner. One explanation for these results is that GAGs are required for the proper function of the epithelial cell receptors that mediate the adherence and endocytosis of *C. albicans*. For example, it has been reported that glycosylation is necessary for the proper function of both EGFR and E-cadherin[48–50], which are key epithelial cell receptors for *C. albicans*[51,52]. Also, sulfated GAGs on the epithelial cell surface may bind to various *C. albicans* proteins[47]. Thus, it is likely that the protective effects of dextran sulfate, both in vitro and in vivo, were due to neutralization of candidalysin, inhibition of epithelial cell receptor function and masking of *C. albicans* surface proteins.

Dextran sulfate not only protected epithelial cells from damage, but also diminished signalling through EGFR, ERK1/2 and c-Fos, leading to reduced release of pro-inflammatory cytokines. As these pathways are activated by candidalysin, it is probable that this inhibition was due in part to neutralization of candidalysin by dextran sulfate. It has also been reported that heparin-binding epidermal growth factor-like growth factor activates EGFR in a paracrine manner and that this activation can be blocked by heparin[48]. Thus, it is possible that dextran sulfate also inhibited epithelial cell stimulation by directly blocking EGFR activation, similarly to heparin.

A central finding was that in the mouse model of vulvovaginal candidiasis, dextran sulfate decreased intravaginal cell damage, cytokine levels and neutrophil accumulation but had no effect on fungal burden. A similar pattern has been seen in mice infected with the candidalysin-deficient *ece1*Δ/Δ mutant[33], providing additional evidence that the salutary effects of dextran sulfate are due at least in part to neutralization of candidalysin. However, it is also likely that dextran sulfate inhibited the pathogenic interactions of *C. albicans* with vaginal epithelial cells by additional mechanisms, such as inhibiting *C. albicans* invasion.

In summary, our study elucidates the intricate relationship between candidalysin and cell surface GAGs, uncovering specific host factors that are required for maximal candidalysin-induced damage. The protective effects of exogenous GAGs, particularly dextran sulfate, present novel therapeutic avenues for mitigating the impact of *C. albicans* infection. These findings contribute to our understanding of the molecular mechanisms underlying candidalysin-induced damage and open new possibilities for targeted antifungal interventions.

Methods

Fungal strains

C. albicans SC5314 was used as the wild-type strain. The candidalysin-deficient *ece1*Δ/Δ mutant was constructed as described[53]. The organisms were grown overnight in yeast extract, peptone, dextrose (YPD) broth at 30 °C in a shaking incubator. The next day, the yeast-phase

organisms were collected through centrifugation, washed twice with PBS, enumerated with a haemacytometer and then resuspended in tissue culture medium.

Candidalysin

Candidalysin (NH_2-SIIGIIMGILGNIPQVIQIIMSIVKAFKGNK-COOH) was produced by solid-phase peptide synthesis using F-MOC chemistry (BioMatik). It was purified to >95% purity by reverse-phased high-performance liquid chromatography. Authentication of sequence and molecular mass (3,311.7 Da (g mol^{-1})) were achieved using liquid chromatography mass spectroscopy. Stock solutions of 10 mM candidalysin were prepared in pure water and stored at −80 °C.

To label candidalysin with CFSE, 10 µl of 10 mM candidalysin in water was mixed with 90 µl DMSO to create a 1 mM candidalysin stock. Next, CFSE (Biolegend, number 423801) was added to the 1 mM candidalysin stock at a final concentration of 5 µM. The mixture was vortexed and then incubated in the dark at room temperature for 20 min. After the labelled candidalysin was prepared, 10 µl was mixed with 1 ml of serum-free, supplement-free medium and then incubated with TR146 cells on glass coverslips in a 24-well plate for various times. The cells were then fixed with paraformaldehyde before subsequent immunofluorescence staining.

Cell culture

The TR146 human buccal epithelial squamous cell carcinoma cells (MilliporeSigma)[54] were incubated in DMEM/F12 medium (Gibco, number 11320033) with 10% fetal bovine serum and 1× penicillin–streptomycin (Gibco, number 15140122). The A431 vulval epithelial cells (MilliporeSigma) and HEK-293T cells (ATCC) were cultured in DMEM medium supplemented with 10% heat-inactivated fetal bovine serum and 2 mM glutamine (Corning, number 25005-CL). The cells were switched to serum-free medium the day before the experiments.

Antibodies and reagents

Mouse anti-Cas9 (number sc517386), mouse anti-hGBF1 (number sc136240), mouse anti-c-Fos (number sc8047), mouse anti-hB3GAT3 (number sc390526) and mouse anti-hXYLT2 (number sc374134) antibodies were purchased from Santa Cruz Biotechnology, and mouse anti-heparan sulfate antibody (clone F58-10E4, number 3702551) was ordered from AMSBIO. Rabbit anti-phospho-c-Fos (Ser32, number 5348), rabbit anti-phospho-EGFR (Tyr1068, number 2234), rabbit anti- EGFR (number 4267), rabbit anti-phospho-ERK1/2 (Thr202/Tyr204, number 4370), rabbit anti-ERK1/2 (number 4695) and rabbit anti-GAPDH (number 5174) were from Cell Signaling. Rabbit anti-hB3GALT6 antibody (number 55049-1-AP) was from ProteinTech, rabbit anti-hSLC39A9 antibody (number PA5-75557) was from Invitrogen and rabbit anti-EMP1 antibody (number bs-0558r) was from Bioss Antibodies. Cross-adsorbed goat anti-mouse IgG-HRP (number G21040), goat anti-rabbit IgG-HRP (number G21234) and goat anti-mouse IgM-Alexa568 (number A21043) were purchased from Invitrogen.

Dextran sulfate sodium salt (6.5–10 kDa, number 441490050) was purchased from Scientific Chemicals. Heparan sulfate (number S5992) and chondroitin sulfate (number S2416) were from Selleck Chemicals LLC. Dextran (60–90 kDa, MP Biomedicals, number 0218014010), dextran sulfate sodium salt (36–50 kDa, MP Biomedicals, number 0216011001), heparin sodium salt (MP Biomedicals, number 0219411450) and alginic acid sodium salt (High Viscosity, number 02154723) were from MP Biomedicals. Dextran (40 kDa, MilliporeSigma, number 31389), dextran (450–650 kDa, MilliporeSigma, number 31392), dextran sulfate sodium salt (>500 kDa, MilliporeSigma, number D6001), alpha-cyclodextrin (MilliporeSigma, number C46421G), alpha-cyclodextrin sulfated sodium salt (MilliporeSigma, number 4945425G) and hyaluronic acid sodium salt (MilliporeSigma, number 53747) were purchased from MilliporeSigma.

Lentivirus preparation and host cell transduction

Lentiviral transductions were performed as previously described[55–57]. Briefly, HEK-293T cells were transfected with the lentiviral packaging plasmids psPAX2 (Addgene, number 12260) and pCMV-VSVG (Addgene, number 8454), along with the appropriate cargo plasmid using the XtremeGene9 transfection reagent (MilliporeSigma, number 30353-5182) in accordance with the manufacturer's instructions. After 48 h, the HEK-293T culture supernatant was collected, filtered through a 0.45 µm PVDF filter (Millipore, number slhv033rs) and added to target TR146 cells cultured to 70–80% confluency in six-well plates. The TR146 cells were infected by adding polybrene (MilliporeSigma, number H9268) to the medium at a final concentration of 4 µg ml^{-1} and centrifuging the tissue culture plates at 1,000 × *g* for 30–60 min at 30 °C. Two days after infection, puromycin was added to the medium and maintained for 7 days to select for transduced cells.

Construction of Cas9-expression TR146 cells

The TR146 cells were transduced with lentivirus that carried the spCas9-Blast construct (Addgene, number 52962) at a multiplicity of infection (MOI) = 0.3 as described above. Two days post-transduction, the TR146 cells were incubated in selective medium containing 5 µg ml^{-1} of blasticidin (Gibco, number A1113903) for 7 days. Cas9 expression in single-cell-derived colonies was confirmed by immunoblotting with an anti-Cas9 antibody. A few clones were further tested in cell damage and uptake assay (Extended Data Fig. 1) to verify that the Cas9-expression TR146 cells were comparable to the wild-type TR146 cells.

Genome-wide CRISPR–Cas9 screening with candidalysin

The TR146 CRISPR genome-wide knockout library was generated using the Brunello human whole genome sgRNA library (Addgene, number 73178)[18,58,59]. This library contains a total of 76,441 sgRNAs with 4 sgRNAs per gene and 1,000 control sgRNAs. The sgRNA library was transduced into TR146–Cas9 cells at an MOI ~0.3. For selection of transduced cells, puromycin (Thermo Scientific, number J672368EQ) was added to the medium at a final concentration of 0.4 µg ml^{-1}. A total of 60 million cells were transduced, ensuring that each sgRNA was represented ~200 times. For screening, the transduced cells were exposed to 30 µM of synthetic candidalysin (Biomatik, de novo synthesized) in serum-free DMEM/F12. Control cells incubated in medium alone were processed in parallel. After 8 h of candidalysin exposure, the surviving cells were rinsed and passaged twice in fresh candidalysin-free medium. This process was repeated five times on two separate occasions. The cells from the last round were expanded and collected, after which their genomic DNA was extracted using the Quick-DNA Midiprep Plus Kit (ZYMO Research, number D4075). DNA fragments containing the sgRNA sequences were amplified by PCR using primers lentiGuidePCR1-F (AATGGACTATCATATGCTTACCGTAACTTGAAAGTATTTCG) and lentiGuidePCR1-R (GTCTGTTGCTATTATGTCTACTATTCTTTCCCCTGCACTG) and purified with CleanNGS SPRI Beads (Bulldog Bio, number CNGS050) according to the manufacturer's instructions. Next-generation sequencing (Illumina HiSeq) was performed by Novogene. The sequencing results were analysed on the web platform PinAPL-Py (http://pinapl-py.ucsd.edu/)[20]. The original sequencing data were deposited to the NCBI under BioProject PRJNA1081917.

Construction of TR146 cells with targeted gene disruptions

All sgRNA oligonucleotides (Extended Data Table 1) were obtained from MilliporeSigma and cloned into the pLentiGuide-Puro plasmid (Addgene, number 53963) as previously described[55,56]. Briefly, pLentiGuide-Puro was digested with BmsBI (Fermentas) and purified using the GeneJET gel extraction kit (Thermo Scientific, number K0692). Subsequently, each pair of oligonucleotides was annealed and phosphorylated with T4 PNK (New England Biolabs, number M0201) following the manufacturer's instructions. The annealed oligonucleotides were ligated with the BsmBI-digested pLentiGuide-Puro plasmid,

which was then validated by PCR and Sanger DNA sequencing. Each pLentiGuide-Puro containing sgRNA was packed into lentivirus and transduced into TR146–Cas9 cells as described above. After 1 week of selection with puromycin, disruption of the targeted gene was verified by immunoblotting with antibodies directed against the corresponding gene product.

siRNA of *GBF1* and *TYK2*

TR146 cells grown in antibiotic-free media at ~70% confluence in a six-well plate were transformed with lipofectamine RNAiMAX reagent (Invitrogen, number 13778) according to the manufacture's protocol. Twenty nanomolar *GBF1* siRNA (Santa Cruz Biotechnology, number SC-105388), tyk2 siRNA (Santa Cruz Biotechnology, number SC-36764) or control scramble siRNA (Santa Cruz Biotechnology, number SC-37007) was applied to TR146 cells twice (time 0 h and time 24 h). Forty-eight hours post-transfection, the cells in supplement-free media were seeded into a 48-well plate overnight for the cell damage assay (time 64 h post-transfection). The total protein of transfected cells was also collected at 64 h for immunoblotting to confirm the successful knockdown of Gbf1 and Tyk2.

Cell survival assay

The susceptibility of the host cells to damage by candidalysin and live *C. albicans* was determined using an XTT assay. The night before the experiment, host cells were seeded into a 48-well tissue culture plate in supplement-free medium. The next day, the cells were rinsed with warm PBS and then incubated with varying concentrations of candidalysin in serum-free DMEM/F12 medium (for TR146 cells) or DMEM medium (for A431 cells) for 6 h. When inhibitors were used, they were added to the host cells either immediately before the candidalysin when the GAGs and GAG analogues were tested or 1 h before the candidalysin when the Tyk2 inhibitors deucravacitinib (3 μM, Selleck Chemicals, number S8879) and TCJL37 (1 μM, Tocris Bioscience, number 6125) were tested. All inhibitors remained in the tissue culture medium for the duration of the experiment, and host cells exposed to the inhibitors in the absence of candidalysin were processed in parallel. At the end of the incubation period, the medium above the cells was aspirated and replaced with phenol-red-free DMEM/F12 medium containing XTT (ATCC, number 30-1011K). After a 60 min incubation, 150 μl of the supernatant was transferred to a clean 96-well plate for measuring OD_{475nm} and OD_{660nm}. The percentage of cells surviving was calculated relative to cells that were not incubated with candidalysin. The percentage protection by the inhibitors was calculated using the following formula: 100 × (sample − candidalysin)/(100 − candidalysin).

The susceptibility of the host cells to damage by *C. albicans* was determined similarly except that the host cells were infected with *C. albicans* at an MOI of 5 for TR146 cells. After 6 h of infection for TR146 cells, the medium was replaced with serum-free medium containing 2 μg caspofungin per ml and the cells were incubated in this medium for 2 h to kill the *C. albicans* cells before performing the XTT assay. All experiments were repeated three times, with two to three replicates each.

In some experiments, an LDH-Cytox assay (Biolegend, number 426401) was used to measure epithelial cell damage. In these experiments, the epithelial cells were grown in a 96-well plate and processed according to the manufacturer's directions. The spontaneous LDH release was determined using uninfected cells that were processed in parallel (untreated). To determine the maximum LDH release (maxLDH), uninfected cells were lysed with 0.5% Triton X-100. Cell damage was calculated as follows: 100 × (treated − untreated)/(maxLDH − untreated).

Immunoblot analysis

TR146 cells were seeded into each well of a 24-well plate (2×10^5 cells per ml) the night before the experiment. The next day, they were incubated with either 10 μM candidalysin or *C. albicans* at an MOI = 5 for various times. After the medium above the cells was aspirated, the epithelial cells were lysed with 2× Laemmli sodium dodecyl sulfate–polyacrylamide gel electrophoresis (SDS–PAGE) sample buffer and the cell lysates were then incubated at 95 °C for 5–10 min. The lysates were resolved by SDS–PAGE, transferred to Immobilon-P PVDF membranes using the wet transfer method and probed with specified antibodies at 4 °C for overnight. After three 10 min washes with PBST, the membrane was incubated with goat anti-mouse or goat anti-rabbit IgG-HRP secondary antibody in 5% fat-free milk at room temperature for 45–60 min. Antigen signals were detected using Radiance Plus substrate (Azure Biosystems, number AC2103) and were visualized and imaged using a C400 imager (Azure Biosystem).

Surface plasmon resonance assays

The GAGs used were porcine intestinal heparin (16 kDa) and porcine intestinal heparan sulfate (12 kDa, Celsus Laboratories), chondroitin sulfate A (20 kDa) from porcine rib cartilage (MilliporeSigma), dermatan sulfate (also known as chondroitin sulfate B, 30 kDa, from porcine intestine, MilliporeSigma), and chondroitin sulfate C (20 kDa, from shark cartilage, MilliporeSigma). *N*-desulfated heparin (14 kDa) and 2-*O*-desulfated heparin (13 kDa) were prepared as described previously[60]. 6-*O*-desulfated heparin (13 kDa) was provided by L. Wang (University of South Florida). Sensor streptavidin (SA) chips were from Cytiva, and surfaced plasmon resonance measurements were performed on a BIAcore 3000 operating with BIAcore 3000 control and BIAevaluation software (version 4.0.1; Cytiva).

The heparin-coated biosensor chip was prepared as previously described[61]. Briefly, heparin was biotinylated by mixing 2 mg heparin and 2 mg amine-PEG3-Biotin (Thermo Scientific), followed by the addition of 10 mg $NaCNBH_3$. After incubation at 70 °C for 24 h, another 10 mg $NaCNBH_3$ was added, and the mixture was incubated at 70 °C for another 24 h. The final product was desalted using a spin column (3,000 molecular weight cut-off) and then lyophilized. The biotinylated heparin was immobilized on a streptavidin chip following the manufacturer's protocol, in which a 20 μl solution of the biotinylated heparin (0.1 mg ml^{-1}) in HBS-EP buffer (0.01 M HEPES, 0.15 M NaCl, 3 mM EDTA, 0.05% surfactant P20, pH 7.4) was injected over flow cell 2 (FC2) of the SA chip at a flow rate of 10 μl min^{-1}. Successful immobilization of heparin was confirmed by the observation of an ~200 resonance unit (RU) increase in the sensor chip. The control flow cell (FC1) was prepared by a 1 min injection with saturated biotin in HBS-EP buffer.

To measure the kinetics of the candidalysin–heparin interaction, candidalysin samples were diluted in HBS-EP buffer. Different dilutions of candidalysin were injected at a flow rate of 30 μl min^{-1}. At the end of the sample injection, HBS-EP buffer was passed over the sensor surface to facilitate dissociation. After a 3 min dissociation time, the sensor surface was regenerated by injecting 30 μl of 0.25% SDS. The response (RU) was monitored as a function of time (sensorgram) at 25 °C.

To test the inhibition of the candidalysin–heparin interaction by other GAGs and chemically modified heparins, candidalysin at 5 μM was pre-mixed with 10 μg ml^{-1} of GAG or 1 μM of chemical modified heparin and injected over the heparin chip at a flow rate of 30 μl min^{-1}. After each run, a dissociation period and regeneration protocol were performed as described above.

Flow cytometry

To measure calcium flux, TR146 cells and *B3GAT3*$^{-/-}$ cells at 1×10^6 cells per ml were loaded with the calcium probe Indo-1/AM (4 μM, Biotium, number 500431) for 30 min at 37 °C in cell loading medium (CLM, DMEM/F12 + 2% heat-inactivated fetal bovine serum + 25 mM HEPES) containing 1 mM EGTA. Cells were washed twice and kept at 37 °C in CLM at a concentration of 1×10^6 cells per ml for another 30 min before flow cytometry. Calcium flux measurements were performed on a FACSymphony A5 cytometer (BD Biosciences) as suggested by the manufacturer. After a baseline Indo-1 fluorescence was recorded

for 90 s, cells were treated with 1 µM of calcium ionophore A23187 (Sigma-Aldrich, number C7522) or 10 µM of candidalysin while cell acquisition continued. Acquisition was performed for an additional 6 min after treatment. The calcium flux was calculated as the ratio of fluorescence intensity at 395 nm (Ca^{2+} bound) and 496 nm (Ca^{2+} free), and followed over time. A kinetic analysis was performed using FlowJo software, and the normalized (to the baseline) smoothed means of fluorescence ratios were plotted.

To quantify the levels of cell surface heparan sulfate, 1×10^6 of TR146, *XYLT2*$^{-/-}$, *B3GALT6*$^{-/-}$ and *B3GAT3*$^{-/-}$ cells were fixed with 4% of paraformaldehyde for 10 min and then blocked with 5% goat serum for 30 min before a 1 h incubation with a primary anti-heparan sulfate antibody (clone F58-10E4, number 3702551) at 1:100 in FACS buffer (PBS + 5% FBS). After the cells were washed three times with FACS buffer, they were incubated with goat anti-mouse IgM-Alexa633 (number A21046) at 1:100 in FACS buffer for 1 h. Cell surface heparan sulfate was quantified using a FACSymphony A5 cytometer, and the results were analysed with FlowJo software.

C-laurdan emission assay

C-laurdan (Tocris, number 7273) was dissolved in chloroform to 1.1025 mM (e = 12,200 M^{-1} cm^{-1}) and further diluted with 200 proof ethanol to create a 100 µM stock suspended in a 91% ethanol and 9% chloroform solution. Samples were prepared in an aqueous buffer (150 mM NaCl, 10 mM HEPES) and incubated with either dextran sulfate (>500 kDa, MilliporeSigma, number D6001) or heparin (Tocris, number 2812) prepared in ultrapure water. Samples with and without candidalysin were loaded into a black 96-well plate (Corning) with 1 µM C-laurdan. The emission spectra from 400 nm to 600 nm were read on a Cytation 5 plate reader (BioTek) using an excitation wavelength of 350 nm. Spectral blanks without dye were subtracted. GP values were calculated using the following equation: $GP = (I_{blue} - I_{red})/(I_{blue} + I_{red})$, where I_{blue} is the summation of fluorescence intensity values within the emission range of 420–460 nm and I_{red} is the summation of fluorescence intensity values within the emission range of 470–510 nm.

Fluorescent dye release assay

Fluorescent dye release experiments were performed as described previously[4]. In brief, lipid films of POPC (Avanti Polar Lipids) were rehydrated with 50 mM calcein solubilized in 50 mM EDTA and 50 mM NaPi (pH 8). Large unilamellar vesicles (LUVs) were formed by extrusion through a 100 nm filter, purified using a PD-10 desalting column (GE Life Sciences) and diluted to a working concentration of 144 µM. GAGs were suspended in MilliQ H_2O at 50 mg ml^{-1} and 5 mg ml^{-1} and mixed with LUVs before measurement. Candidalysin suspended at 0.72 µM in candidalysin buffer (150 mM NaCl and 10 mM HEPES) was incubated with GAG + LUVs at a lipid to peptide molar ratio of 200:1 at the time of measurement in a 96-well black plate. Fluorescent readings were taken on a Cytation 5 plate reader using an excitation wavelength of 495 nm and an emission wavelength of 515 nm. Measurements were collected for 2 h.

Atomic force microscope imaging

Candidalysin was hydrated in deionized water to 100 µM. The stock solution was divided into 10 µl aliquots and stored at −80 °C. DOPC stock in chloroform (Avanti Polar Lipids) was dried under argon gas and vacuum overnight. Lipid films were resuspended in imaging buffer (10 mM HEPES, 150 mM NaCl, pH 7.3) and extruded through 100 nm filters (Whatman) to form LUVs using a mini-extruder (Avanti Polar Lipids). The solution was aliquoted and stored at −80 °C. Lipid concentration was determined using a standard phosphorus assay[62]. For control experiments, a candidalysin aliquot was thawed and diluted to 333 nM in imaging buffer. The samples were incubated at 25 °C for 30 min; then 90 µl was deposited onto freshly cleaved mica discs (Ted Pella) and incubated for an additional 10 min. Loosely bound particles were washed away via buffer exchange (90 µl of buffer exchanged across the sample five to six times). Control experiments were also conducted to visualize candidalysin pores in DOPC in the absence of GAGs. These samples were prepared in a manner that replicated the previous control incubation experiments. A candidalysin aliquot was thawed and diluted to 555 nM in imaging buffer and incubated at 25 °C. After 20 min, candidalysin was mixed with DOPC such that the final concentrations were 333 nM candidalysin and 200 µM DOPC. The solution was incubated for 10 min to allow candidalysin to interact with liposomes; then 90 µl was deposited on mica. Samples were incubated for another 10 min to allow lipid vesicles to rupture and form bilayers. The lipid samples were rinsed via buffer exchange as before. Images were collected in imaging buffer with biolever mini tips (Olympus, k ~0.1 N m^{-1}, f_o ~30 kHz in fluid) on a commercial instrument using tapping mode (Cypher, Asylum Research). Tip-sample forces were kept below 100 pN to reduce the likelihood of protein deformation.

To image candidalysin in the presence of GAGs, dextran, dextran sulfate or heparan sulfate was diluted from stock concentrations in the imaging buffer. Each solution was mixed with candidalysin such that the final carbohydrate concentration was 5 µg ml^{-1} and the candidalysin concentration was 333 nM. The samples were incubated for 30 min at 25 °C; then, 90 µl was deposited on freshly cleaved mica and incubated for an additional 10 min. The sample was washed via buffer exchange, then imaged. When imaging candidalysin and GAGs with lipid, candidalysin and GAG stocks were mixed and incubated for 20 min. This solution was then added to DOPC such that the final concentrations were 333 nM candidalysin, 5 µg ml^{-1} carbohydrate and 200 µM DOPC. This mixture was incubated an additional 10 min; then, 90 µl was deposited on freshly cleaved mica and incubated for another 10 min to allow lipid bilayer formation. The sample was rinsed via buffer exchange and imaged. Image flattening and analysis were performed using a commercial software package (Asylum Research). Loop and pore counts were done manually.

Transmission electron microscope imaging

TEM was performed using 3 µM candidalysin samples incubated for 30 min in imaging buffer (10 mM HEPES, 150 mM NaCl, pH 7.3) at 25 °C. Five microlitre droplets were then incubated on carbon grids (Electron Microscopy Sciences) for 2 min at 25 °C and negatively stained with uranyl acetate. For candidalysin in the presence of GAGs, samples contained 3 µM candidalysin and 50 µg ml^{-1} of dextran, dextran sulfate or heparan sulfate and were incubated for 30 min at 25 °C. TEM grids for these samples were prepared as described[4]. Grids were imaged at 120 kV (JEOL, JEM-1400).

Immunofluorescence microscopy

Epithelial cells grown on 12 mm round glass coverslips (Chemglass Life Sciences, number CLS1763012) were incubated with candidalysin for various times and then fixed with 4% paraformaldehyde in PBS for 10 min at room temperature. After the cells were blocked with 0.1% BSA or 5% goat serum in PBS for 1 h, they were incubated in primary antibody diluted in PBS + 0.1% BSA for 1 h. The coverslips were washed and then stained for 1 h with fluorophore-conjugated secondary antibody and/or DAPI (MilliporeSigma, number MBD0015) in the dark. They were mounted inverted onto glass slides using ProLong Gold Antifade Reagent (Cell Signaling, number 9071) and sealed with nail polish before imaging with an Olympus IX83 fluorescence microscope. The number of CFSE-labelled candidalysin aggregates was counted manually. The colocalization of fluorescent signals was analysed with the built-in modules in the CellSens Olympus microscope software 3.1 (build 21199).

Epithelial invasion assay

C. albicans invasion of epithelial cells was determined using a differential fluorescence assay as described previously[52,57,63]. Briefly, TR146 epithelial cells were grown on glass coverslips the day before infection and

then infected with *C. albicans* blastospores at an MOI of 1 for 90 min. The cells were rinsed in a standardized manner and then fixed with 4% paraformaldehyde. The non-endocytosed fungal cells were stained for 1 h with a rabbit anti-*Candida* antibody labelled with Alexa568. After the epithelial cells were rinsed with PBS, they were permeabilized for 15 min in 0.1% Triton X-100 in PBS and the endocytosed and non-endocytosed fungal cells were stained with a rabbit anti-*Candida* antibody labelled with Alexa488. The coverslips were rinsed with PBS, mounted inverted on microscopic slides and visualized using epifluorescence microscopy. The percentage of invading *C. albicans* cells was determined by dividing the number of internalized cells by the total number of fungal cells per high-power field, and normalized to the controls. A minimum of 100 fungal cells were counted on each coverslip.

Cytokine assays

Host cells grown in 48-well plates were incubated with either 10 µM candidalysin or *C. albicans* at an MOI of 5 as in the cell survival experiments. After 6 h and 24 h for TR146 and A431 cells, respectively, the culture supernatant was collected and stored at −20 °C. Later, the concentration of IL-1β (R&D, number DY20105; BD, number 557953), GM-CSF (BD, number 555126) and CXCL8 (BD, number 555244) in the conditioned medium was measured by ELISA according to the manufacturer's instructions.

Mouse model of VVC

The mouse model of VVC was performed as described previously with slight modifications[64–66]. Groups ($n = 7$) of 6–8-week-old female C57BL/6 and CD-1 mice were purchased from Charles River Laboratories and housed in isolator cages mounted on ventilated racks. The mice were administered 0.1 mg β-oestradiol 17-valerate (MilliporeSigma, number E1631-1G) dissolved in sesame oil subcutaneously 3 days before vaginal lavage or challenge with *C. albicans*. Stationary-phase cultures of *C. albicans* strain SC5314 were washed and adjusted to 5×10^8 cells per ml in sterile endotoxin-free PBS. Mice were intravaginally inoculated with 10 µl of cell suspension, generating an inoculum size of 5×10^6 blastospores. Colitis-grade dextran sulfate sodium salt (DSS; number 160110, MP biomedicals) was dissolved with sterile cell-culture-grade water to 5 mg ml^{-1}, then mixed with carboxymethylcellulose sodium salt (CMC, Millipore, number 217274-250GM) to make a 3% CMC gel. Vehicle (VEH) was composed of unsupplemented 3% CMC gel. Mice were intravaginally administered 20 µl of 5 mg ml^{-1} DSS or VEH gel formulation every 24 h from day −1 until day 2 post-inoculation (p.i.). At day 3 p.i., mice were killed and vaginal lavage fluids (VLF) were obtained by flushing the vaginal canal with 100 µl of PBS.

Assessment of fungal burden

Recovered VLFs were spiked with 1× final cOmplete Mini EDTA-free Protease Inhibitor (Roche, number 11836170001). Fresh VLF (10 µl) was smeared onto Tissue Path Superfrost Plus Gold slides (Fisher Scientific), air-dried, fixed with CytoPrep fixative (Fisher Scientific) and stored at room temperature. VLF were centrifuged at 4,000 rpm, and the supernatant was transferred for storage at −80 °C. Cell pellets were resuspended in their original volume of PBS as assessed by weight. An aliquot was serially diluted, plated on YPD agar plates containing 50 µg ml^{-1} chloramphenicol (number BP904-100, Fisher Scientific) and subsequently incubated at 30 °C for 48 h (ref. 67). The resulting colonies were enumerated and log transformed as a measure of fungal burden. The Papanicolaou technique was used to assess polymorphonuclear leucocyte (PMN) recruitment by manually counting five nonadjacent fields by standard light microscopy using a ×40 objective and reported as the mean. The cytokine IL-1β was measured using ELISA (Invitrogen, number 88-7013A-88) according to the manufacturer's instruction. The ToxiLight Non-destructive Cytotoxicity BioAssay (Lonza, number 186467) was used to measure adenylate kinase release in vaginal lavage fluid as a measure of tissue damage per the manufacturer's instructions. Luminescence values were quantitated using a Synergy H1 microplate reader (Biotek).

Ethics statement

The animals used in this study were housed in Association for Assessment and Accreditation of Laboratory Animal Care-approved facilities located in the Regional Biocontainment Laboratory (RBL) at the University of Tennessee Health Science Center (UTHSC). The animal work conducted in this study was approved by the UTHSC Institutional Animal Care and Use Committee under protocol 21-0265 in accordance with the Guide for the Care and Use of Laboratory Animals. Every effort was taken to ensure that the use of animals was necessary for hypothesis testing, that the minimum number of animals required was used and that steps were taken to minimize discomfort. Mice were given standard rodent chow and water ad libitum and monitored for signs of distress, including noticeable weight loss and lethargy.

Reporting summary

Further information on research design is available in the Nature Portfolio Reporting Summary linked to this article.

Data availability

The original sequencing data were deposited in NCBI under BioProject PRJNA1081917. All data from this study are presented in the Article and the extended data figures and table. Source data are provided with this paper.

References

1. Moyes, D. L. et al. Candidalysin is a fungal peptide toxin critical for mucosal infection. *Nature* **532**, 64–68 (2016).
2. Swidergall, M. et al. Candidalysin is required for neutrophil recruitment and virulence during systemic *Candida albicans* infection. *J. Infect. Dis.* https://doi.org/10.1093/infdis/jiz322 (2019).
3. Ho, J. et al. Candidalysin activates innate epithelial immune responses via epidermal growth factor receptor. *Nat. Commun.* **10**, 2297 (2019).
4. Russell, C. M. et al. The *Candida albicans* virulence factor candidalysin polymerizes in solution to form membrane pores and damage epithelial cells. *eLife* https://doi.org/10.7554/eLife.75490 (2022).
5. Naglik, J. R., Gaffen, S. L. & Hube, B. Candidalysin: discovery and function in *Candida albicans* infections. *Curr. Opin. Microbiol.* **52**, 100–109 (2019).
6. Swidergall, M. et al. EphA2 is a neutrophil receptor for *Candida albicans* that stimulates antifungal activity during oropharyngeal infection. *Cell Rep.* **28**, 423–433 e425 (2019).
7. Westman, J. et al. Calcium-dependent ESCRT recruitment and lysosome exocytosis maintain epithelial integrity during *Candida albicans* invasion. *Cell Rep.* **38**, 110187 (2022).
8. Mogavero, S. et al. Candidalysin delivery to the invasion pocket is critical for host epithelial damage induced by *Candida albicans*. *Cell Microbiol.* **23**, e13378 (2021).
9. Kasper, L. et al. The fungal peptide toxin candidalysin activates the NLRP3 inflammasome and causes cytolysis in mononuclear phagocytes. *Nat. Commun.* **9**, 4260 (2018).
10. Russell, C. M., Rybak, J. A., Miao, J., Peters, B. M. & Barrera, F. N. Candidalysin: connecting the pore forming mechanism of this virulence factor to its immunostimulatory properties. *J. Biol. Chem.* **299**, 102829 (2023).
11. Hanaoka, M. & Domae, E. IL-1α released from oral epithelial cells upon candidalysin exposure initiates an early innate epithelial response. *Int. Immunol.* **33**, 161–170 (2021).
12. Nikou, S. A. et al. The *Candida albicans* toxin candidalysin mediates distinct epithelial inflammatory responses through p38 and EGFR–ERK pathways. *Sci. Signal.* **15**, eabj6915 (2022).

13. Hu, L. et al. Candidalysin amplifies the immune inflammatory response in *Candida albicans* keratitis through the TREM-1/DAP12 pathway. *Int. Immunopharmacol.* **119**, 110195 (2023).
14. Ponde, N. O. et al. Receptor-kinase EGFR–MAPK adaptor proteins mediate the epithelial response to *Candida albicans* via the cytolytic peptide toxin, candidalysin. *J. Biol. Chem.* **298**, 102419 (2022).
15. Moyes, D. L. et al. A biphasic innate immune MAPK response discriminates between the yeast and hyphal forms of *Candida albicans* in epithelial cells. *Cell Host Microbe* **8**, 225–235 (2010).
16. Mori, T., Kataoka, H., Tanabe, G. & Into, T. Solubility affects IL-1β-producing activity of the synthetic candidalysin peptide. *PLoS ONE* **17**, e0273663 (2022).
17. Altmeier, S. et al. IL-1 coordinates the neutrophil response to *C. albicans* in the oral mucosa. *PLoS Pathog.* **12**, e1005882 (2016).
18. Doench, J. G. et al. Optimized sgRNA design to maximize activity and minimize off-target effects of CRISPR–Cas9. *Nat. Biotechnol.* **34**, 184–191 (2016).
19. Sanson, K. R. et al. Optimized libraries for CRISPR–Cas9 genetic screens with multiple modalities. *Nat. Commun.* **9**, 5416 (2018).
20. Spahn, P. N. et al. PinAPL-Py: a comprehensive web-application for the analysis of CRISPR/Cas9 screens. *Sci. Rep.* **7**, 15854 (2017).
21. Yamaji, T. et al. A CRISPR screen using subtilase cytotoxin identifies SLC39A9 as a glycan-regulating factor. *iScience* **15**, 407–420 (2019).
22. Saenz, J. B. et al. Golgicide A reveals essential roles for GBF1 in Golgi assembly and function. *Nat. Chem. Biol.* **5**, 157–165 (2009).
23. Lindahl, U., Couchman, J., Kimata, K. & Esko, J. D. in *Essentials of Glycobiology* (eds Varki, A. et al.) 207–221 (Cold Spring Harbor Laboratory Press, 2015).
24. Chen, Y. H. et al. The GAGOme: a cell-based library of displayed glycosaminoglycans. *Nat. Methods* **15**, 881–888 (2018).
25. Mizumoto, S. & Yamada, S. Congenital disorders of deficiency in glycosaminoglycan biosynthesis. *Front. Genet.* **12**, 717535 (2021).
26. Soares da Costa, D., Reis, R. L. & Pashkuleva, I. Sulfation of glycosaminoglycans and its implications in human health and disorders. *Annu. Rev. Biomed. Eng.* **19**, 1–26 (2017).
27. Ritelli, M. et al. Further defining the phenotypic spectrum of B3GAT3 mutations and literature review on linkeropathy syndromes. *Genes* https://doi.org/10.3390/genes10090631 (2019).
28. Aquino, R. S. & Park, P. W. Glycosaminoglycans and infection. *Front. Biosci.* **21**, 1260–1277 (2016).
29. Shi, D., Sheng, A. & Chi, L. Glycosaminoglycan–protein interactions and their roles in human disease. *Front. Mol. Biosci.* **8**, 639666 (2021).
30. Vallet, S. D., Clerc, O. & Ricard-Blum, S. Glycosaminoglycan–protein interactions: the first draft of the glycosaminoglycan interactome. *J. Histochem. Cytochem.* **69**, 93–104 (2021).
31. Levitan, I. Evaluating membrane structure by Laurdan imaging: disruption of lipid packing by oxidized lipids. *Curr. Top. Membr.* **88**, 235–256 (2021).
32. Orlikowska-Rzeznik, H., Krok, E., Chattopadhyay, M., Lester, A. & Piatkowski, L. Laurdan discerns lipid membrane hydration and cholesterol content. *J. Phys. Chem. B* **127**, 3382–3391 (2023).
33. Liu, J. et al. A variant ECE1 allele contributes to reduced pathogenicity of *Candida albicans* during vulvovaginal candidiasis. *PLoS Pathog.* **17**, e1009884 (2021).
34. Valentine, M. et al. Nanobody-mediated neutralization of candidalysin prevents epithelial damage and inflammatory responses that drive vulvovaginal candidiasis pathogenesis. *mBio* https://doi.org/10.1128/mbio.03409-23 (2024).
35. Yano, J., Noverr, M. C. & Fidel, P. L. Jr. Vaginal heparan sulfate linked to neutrophil dysfunction in the acute inflammatory response associated with experimental vulvovaginal candidiasis. *mBio* https://doi.org/10.1128/mBio.00211-17 (2017).
36. Zhou, Y. et al. Sulfated glycosaminoglycans and low-density lipoprotein receptor mediate the cellular entry of *Clostridium novyi* alpha-toxin. *Cell Res.* **31**, 935–938 (2021).
37. Tao, L. et al. Sulfated glycosaminoglycans and low-density lipoprotein receptor contribute to *Clostridium difficile* toxin A entry into cells. *Nat. Microbiol.* **4**, 1760–1769 (2019).
38. Tian, S. et al. Genome-wide CRISPR screens for Shiga toxins and ricin reveal Golgi proteins critical for glycosylation. *PLoS Biol.* **16**, e2006951 (2018).
39. Schneider, W. M. et al. Genome-scale identification of SARS-CoV-2 and pan-coronavirus host factor networks. *Cell* **184**, 120–132.e14 (2021).
40. Wang, R. et al. Genetic screens identify host factors for SARS-CoV-2 and common cold coronaviruses. *Cell* **184**, 106–119. e14 (2021).
41. Labeau, A. et al. A genome-wide CRISPR–Cas9 screen identifies the dolichol-phosphate mannose synthase complex as a host dependency factor for dengue virus infection. *J. Virol.* https://doi.org/10.1128/JVI.01751-19 (2020).
42. Luteijn, R. D. et al. A genome-wide haploid genetic screen identifies heparan sulfate-associated genes and the macropinocytosis modulator TMED10 as factors supporting vaccinia virus infection. *J. Virol.* https://doi.org/10.1128/JVI.02160-18 (2019).
43. Simon Davis, D. A. & Parish, C. R. Heparan sulfate: a ubiquitous glycosaminoglycan with multiple roles in immunity. *Front. Immunol.* **4**, 470 (2013).
44. Zhang, T. Y. et al. Global fungal–host interactome mapping identifies host targets of candidalysin. *Nat. Commun.* **15**, 1757 (2024).
45. Domae, E., Kamada, A., Yoshikawa, Y. & Ikeo, T. Heparin interacts with candidalysin and neutralizes its cytotoxicity to oral epithelial cells. *J. Oral. Biosci.* **65**, 206–210 (2023).
46. Austermeier, S. et al. Albumin neutralizes hydrophobic toxins and modulates *Candida albicans* pathogenicity. *mBio* **12**, e0053121 (2021).
47. Green, J. V. et al. Heparin-binding motifs and biofilm formation by *Candida albicans*. *J. Infect. Dis.* **208**, 1695–1704 (2013).
48. Kalmes, A., Vesti, B. R., Daum, G., Abraham, J. A. & Clowes, A. W. Heparin blockade of thrombin-induced smooth muscle cell migration involves inhibition of epidermal growth factor (EGF) receptor transactivation by heparin-binding EGF-like growth factor. *Circ. Res.* **87**, 92–98 (2000).
49. Azimzadeh Irani, M., Kannan, S. & Verma, C. Role of N-glycosylation in EGFR ectodomain ligand binding. *Proteins* **85**, 1529–1549 (2017).
50. Carvalho, S. et al. O-mannosylation and N-glycosylation: two coordinated mechanisms regulating the tumour suppressor functions of E-cadherin in cancer. *Oncotarget* **7**, 65231–65246 (2016).
51. Zhu, W. et al. EGFR and HER2 receptor kinase signaling mediate epithelial cell invasion by *Candida albicans* during oropharyngeal infection. *Proc. Natl Acad. Sci. USA* **109**, 14194–14199 (2012).
52. Phan, Q. T. et al. Als3 is a *Candida albicans* invasin that binds to cadherins and induces endocytosis by host cells. *PLoS Biol.* **5**, e64 (2007).
53. Swidergall, M. et al. Activation of EphA2–EGFR signaling in oral epithelial cells by *Candida albicans* virulence factors. *PLoS Pathog.* **17**, e1009221 (2021).
54. Rupniak, H. T. et al. Characteristics of four new human cell lines derived from squamous cell carcinomas of the head and neck. *J. Natl Cancer Inst.* **75**, 621–635 (1985).
55. Sanjana, N. E., Shalem, O. & Zhang, F. Improved vectors and genome-wide libraries for CRISPR screening. *Nat. Methods* **11**, 783–784 (2014).

56. Shalem, O. et al. Genome-scale CRISPR–Cas9 knockout screening in human cells. *Science* **343**, 84–87 (2014).
57. Phan, Q. T. et al. The globular C1q receptor is required for epidermal growth factor receptor signaling during *Candida albicans* infection. *mBio* **12**, e0271621 (2021).
58. Joung, J. et al. Genome-scale CRISPR–Cas9 knockout and transcriptional activation screening. *Nat. Protoc.* **12**, 828–863 (2017).
59. Yau, E. H. & Rana, T. M. Next-generation sequencing of genome-wide CRISPR screens. *Methods Mol. Biol.* **1712**, 203–216 (2018).
60. Yates, E. A. et al. 1H and 13C NMR spectral assignments of the major sequences of twelve systematically modified heparin derivatives. *Carbohydr. Res.* **294**, 15–27 (1996).
61. He, P. et al. SPR sensor-based analysis of the inhibition of marine sulfated glycans on interactions between monkeypox virus proteins and glycosaminoglycans. *Mar. Drugs* https://doi.org/10.3390/md21050264 (2023).
62. Stewart, J. C. Colorimetric determination of phospholipids with ammonium ferrothiocyanate. *Anal. Biochem.* **104**, 10–14 (1980).
63. Phan, Q. T. et al. Serum bridging molecules drive candidal invasion of human but not mouse endothelial cells. *PLoS Pathog.* **18**, e1010681 (2022).
64. Peters, B. M. et al. Fungal morphogenetic pathways are required for the hallmark inflammatory response during *Candida albicans* vaginitis. *Infect. Immun.* **82**, 532–543 (2014).
65. Bruno, V. M. et al. Transcriptomic analysis of vulvovaginal candidiasis identifies a role for the NLRP3 inflammasome. *mBio* https://doi.org/10.1128/mBio.00182-15 (2015).
66. Yano, J. & Fidel, P. L. Jr. Protocols for vaginal inoculation and sample collection in the experimental mouse model of *Candida* vaginitis. *J. Vis. Exp.* https://doi.org/10.3791/3382 (2011).
67. Miao, J. et al. Glycogen metabolism in *Candida albicans* impacts fitness and virulence during vulvovaginal and invasive candidiasis. *mBio* **14**, e0004623 (2023).

Acknowledgements

This work was supported in part by grants R01DE026600 (to S.G.F.), R01AI134796 (to B.M.P.), R35GM140846 (to F.N.B.), U01-AI124319 and U19-AI172713 (to M.R.Y.), and S10OD028523 and R21AI156573 (to R.J.L. and F.Z.) from the National Institutes of Health, USA, and 2122027 (to G.M.K.) from the National Science Foundation, USA. J.M. received financial support from the China Scholarship Council award 201906150153 and the UTHSC Center for Pediatric Experimental Therapeutics. K.G.S. acknowledges support from the Research Excellence Program at the University of Missouri. C.M.R. was supported by a Graduate Advancement & Training Education Fellowship from the University of Tennessee—Oak Ridge Innovation Institute. We thank Z.-Q. Koo and Y.-H. Tsai of the Institute of Microbiology and Immunology in Taipei for the detailed protocol for labelling candidalysin with CFSE. The funding agencies had no role in the study design, data collection, data interpretation or preparation of the paper. The elements in our diagrams were adapted from the Servier Medical Art (SMART, https://smart.servier.com/) under CC BY 4.0.

Author contributions

J.L. and S.G.F. initiated and designed the project. S.G.F. secured funding for the project. J.L. carried out the CRISPR–Cas9 screen. J.L. constructed the cell knockouts. M.R.Y. and S.G.F. provided candidalysin, and J.L. performed the candidalysin damage assays, immunofluorescence imaging and immunoblots. Q.T.P. and J.L. did the fungal invasion assays. H.L. and J.L. performed the IL-1β, GM-CSF and CXCL8 ELISAs, flow cytometry and calcium flux assays. M.T. and J.L. did the LDH assays. K.G.S. and G.M.K. performed electron microscopy and AFM imaging. F.Z., J.S.D. and R.J.L. performed the SPR assays and acquired funding. C.M.R., R.J.P. and F.N.B. did the dye release and C-laurdan assays. B.M.P., J.M. and N.V.S. carried out the animal infection experiment and related assays. J.L. and S.G.F. wrote the paper with input, revision and review from all co-authors.

Competing interests

The authors declare no competing interests.

Additional information

Extended data is available for this paper at https://doi.org/10.1038/s41564-024-01794-8.

Supplementary information The online version contains supplementary material available at https://doi.org/10.1038/s41564-024-01794-8.

Correspondence and requests for materials should be addressed to Scott G. Filler.

Peer review information *Nature Microbiology* thanks the anonymous reviewers for their contribution to the peer review of this work. Peer reviewer reports are available.

Reprints and permissions information is available at www.nature.com/reprints.

Publisher's note Springer Nature remains neutral with regard to jurisdictional claims in published maps and institutional affiliations.

[1]Institute for Infection and Immunity, Lundquist Institute for Biomedical Innovation at Harbor-UCLA Medical Center, Torrance, CA, USA. [2]Pharmaceutical Sciences Program, College of Graduate Health Sciences, University of Tennessee Health Science Center, Memphis, TN, USA. [3]Department of Physics and Astronomy, University of Missouri, Columbia, MO, USA. [4]Department of Biochemistry & Cellular and Molecular Biology, University of Tennessee, Knoxville, TN, USA. [5]Genome Science and Technology, University of Tennessee, Knoxville, TN, USA. [6]Department of Chemical and Biological Engineering and Center for Biotechnology and Interdisciplinary Studies, Rensselaer Polytechnic Institute, Troy, NY, USA. [7]Department of Infectious Diseases, Nagasaki University Graduate School of Biomedical Sciences, Nagasaki, Japan. [8]David Geffen School of Medicine at UCLA, Los Angeles, CA, USA. [9]Division of Infectious Diseases, Department of Medicine, Harbor-UCLA Medical Center, Torrance, CA, USA. [10]Division of Molecular Medicine, Department of Medicine, Harbor-UCLA Medical Center, Torrance, CA, USA. [11]Department of Biochemistry, University of Missouri-Columbia, Columbia, MO, USA. [12]Department of Clinical Pharmacy and Translational Science, College of Pharmacy, University of Tennessee Health Science Center, Memphis, TN, USA. [13]Department of Microbiology, Immunology, and Biochemistry, College of Medicine, University of Tennessee Health Science Center, Memphis, TN, USA. ✉e-mail: sfiller@ucla.edu

https://doi.org/10.1038/s41564-024-01794-8

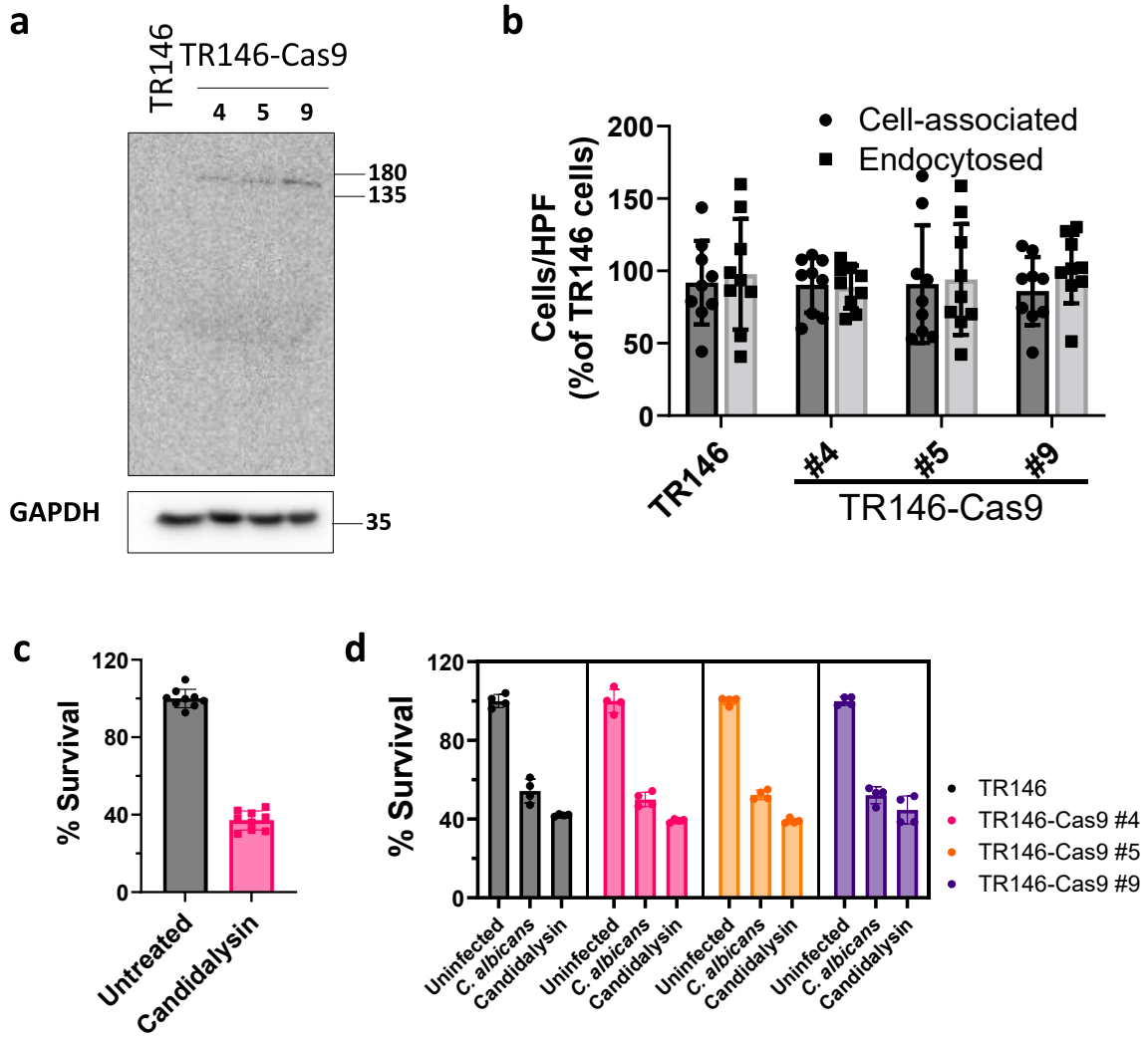

Extended Data Fig. 1 | Cas9-expressing TR146 cells display comparable phenotypes to wild-type TR146 cells in response to wild-type *C. albicans* SC5314 and candidalysin. a, Immunoblots of 3 clones of TR146 cells that stably expressed the $P_{EF\text{-}1\alpha}$-*Cas9-Blasticidin* construct. **b**, *C. albicans* association with and endocytosis by wild-type TR146 cells and the indicated clones of TR146-Cas9 cells. **c**, Survival of TR146 cells in response to a 6-h exposure to 30 μM candidalysin as measured by an XTT assay. **d**, Survival of TR146 cells and TR146-Cas9 clones as measured by an XTT assay after a 6-h exposure to *C. albicans* (multiplicity of infection [MOI] = 5) or candidalysin (30 μM). Clone 4 was selected for use in the subsequent experiments. Results are mean ± SD of 3 (**b, c**) or 2 experiments (**d**), each performed in triplicate (**b, c**) or duplicate (**d**).

https://doi.org/10.1038/s41564-024-01794-8

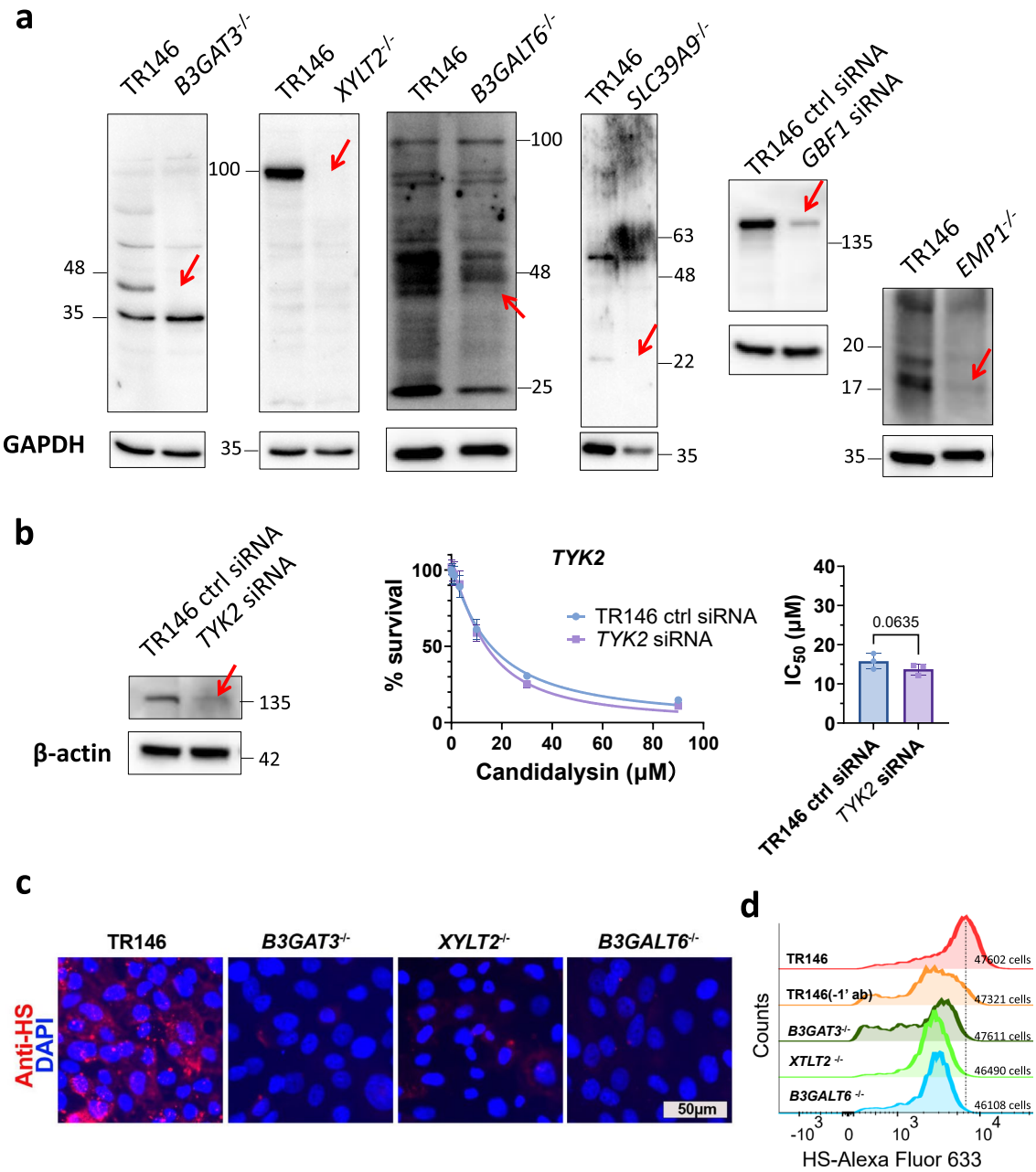

Extended Data Fig. 2 | Immunoblots and immunofluorescence images of gene knockouts and knockdowns. a, Immunoblots for B3gat3, Xylt2, B3galt6, Slc39a9 and Gbf1 in the corresponding CRISPR knockout cells or siRNA knockdown cells. Arrows indicate the target proteins. Numbers indicate molecular mass. **b**, *TYK2* siRNA knockdown does not affect survival of oral epithelial cells after 6-h of candidalysin exposure. The left panel shows a representative Tyk2 immunoblot. The middle panel shows the survival (measured by an XTT assay) of epithelial cells exposed to the indicated concentrations of candidalysin. The plots represent the combined results of 3 experiments, each performed in triplicate. The right panel shows the concentration of candidalysin that yielded 50% survival (IC_{50}), which was calculated from the data in the corresponding graph in the middle panel. Results are mean ± SD. P values were calculated using the unpaired, two-sided Student's t test. **c**, Representative immunofluorescence images of TR146, B3GAT3$^{-/-}$, *XYLT2*$^{-/-}$ and *B3GALT6*$^{-/-}$ cells stained with an anti-heparan sulfate antibody (red) and DAPI (blue) from 3 independent experiments. Scale bar: 50μm. **d**, Flow cytometric analysis of heparan sulfate expression on the surface of TR146 cells and the indicated mutants.

https://doi.org/10.1038/s41564-024-01794-8

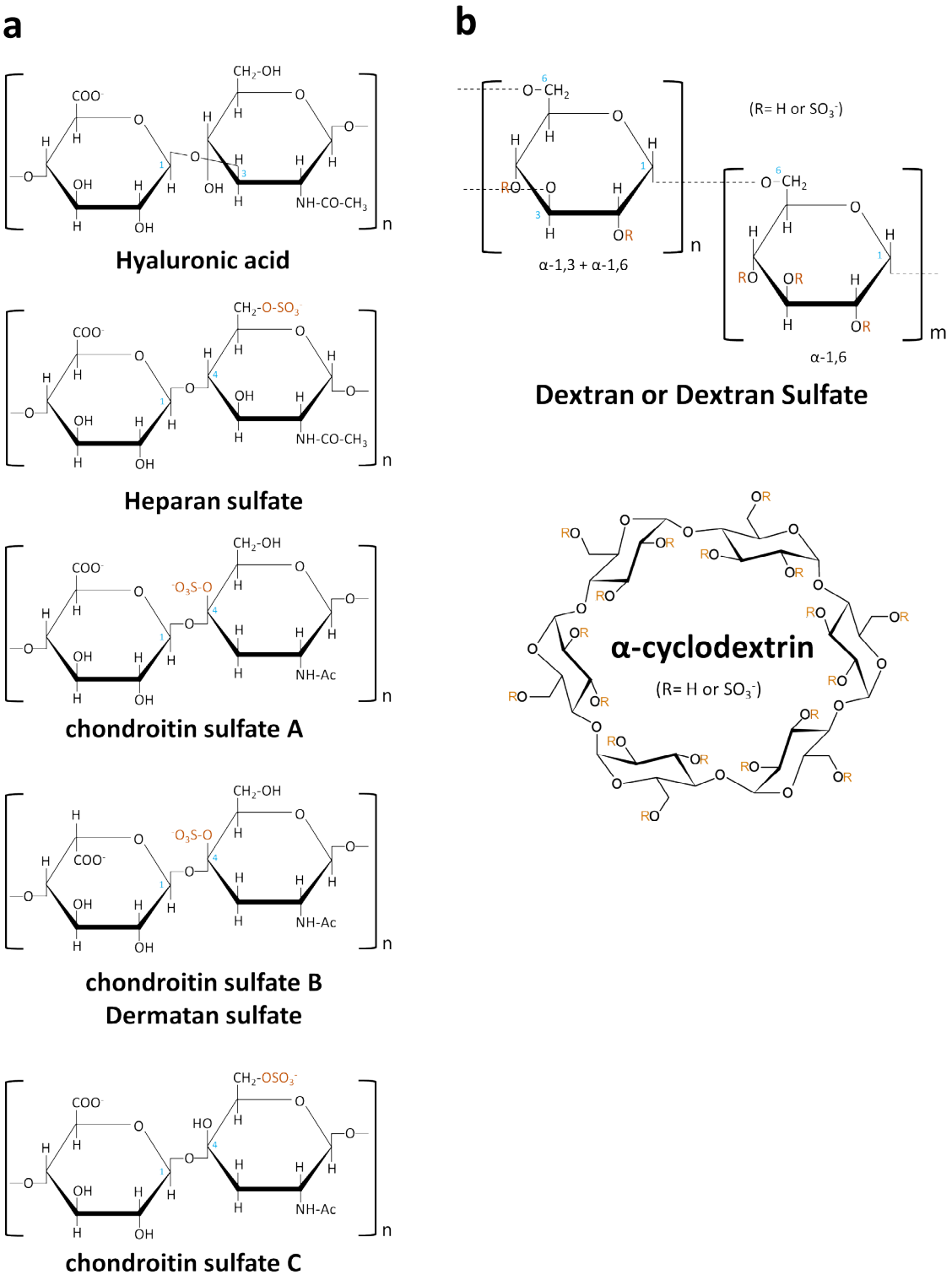

Extended Data Fig. 3 | Structures of GAGs and GAG analogs used in the experiments. a, Structure of the naturally occurring GAGS, hyaluronic acid, heparan sulfate, chondroitin sulfate A, chondroitin sulfate B (dermatan sulfate) and chondroitin sulfate C. **b**, Structure of the GAG analogs dextran/dextran sulfate, and alpha-cyclodextrin/sulfated alpha-cyclodextrin.

https://doi.org/10.1038/s41564-024-01794-8

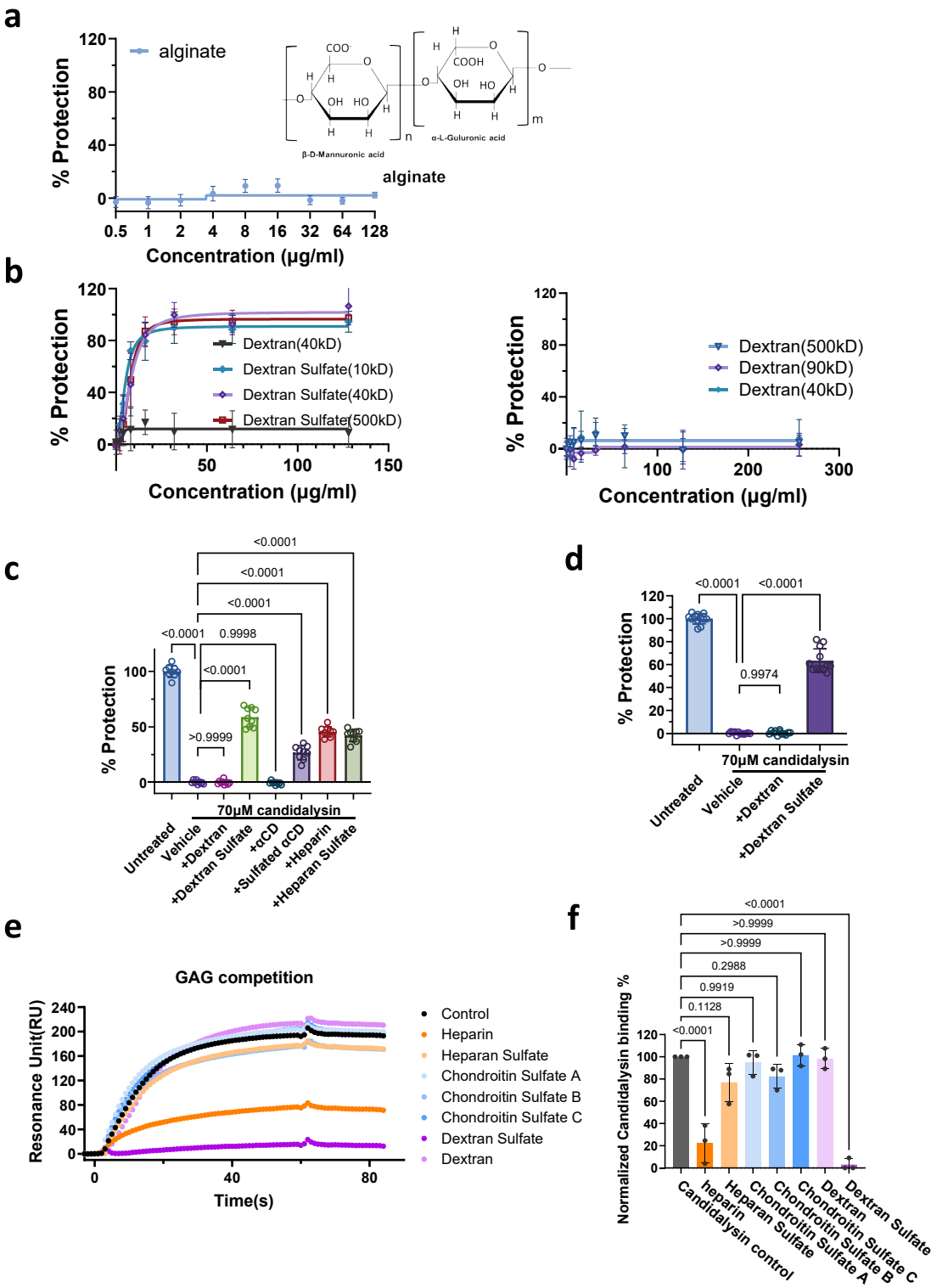

Extended Data Fig. 4 | Sulfated GAGs but not carboxylated or non-sulfated GAGs protect epithelial cells from candidalysin-induced damage. a, Alginate does not protect oral epithelial cells from damage caused by a 6-h exposure to 30 μM candidalysin. **b**, Protection from damage caused by a 6-h exposure to 30 μM candidalysin provided by dextran and dextran sulfate of the indicated molecular masses. **c**, Protection from damage caused by a 6-h exposure to 70 μM candidalysin provided by 100 μg/ml of dextran, dextran sulfate, α--cyclodextrin, sulfated α-cyclodextrin, heparin, and heparan sulfate. **d**, Protection from damage caused by a 24-h exposure to 70 μM candidalysin provided by 100 μg/ml of dextran, and dextran sulfate. **e**, Representative surface plasmon resonance sensorgrams showing the effects of heparin, heparan sulfate, chondroitin sulfate A, chondroitin sulfate B, chondroitin sulfate C, dextran and dextran sulfate on the interaction of candidalysin with heparin on a biosensor chip. **f**, Combined results of 3 independent experiments showing the inhibitory effects of the various GAGs or GAG analogs on the interaction of candidalysin with heparin. Results in **a, b**, and **f** are mean ± SD of 3 independent experiments, and results in **c** and **d** are mean ± SD of 3-4 independent experiments, each performed in triplicate. Protection was determined using an XTT assay. P values were calculated using the one-way ANOVA with Dunnett's multiple comparisons test (**c**, **d**, and **f**).

https://doi.org/10.1038/s41564-024-01794-8

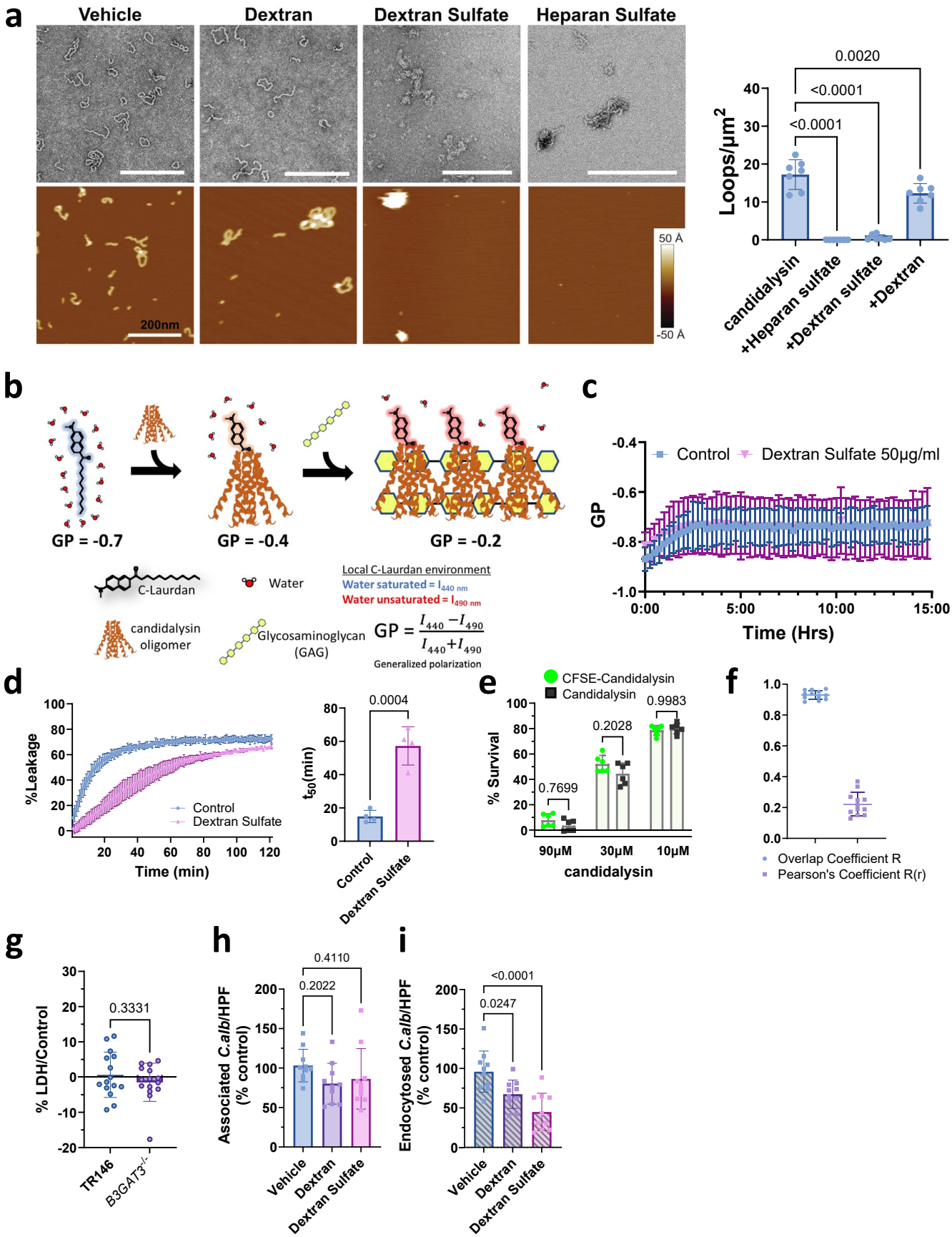

Extended Data Fig. 5 | See next page for caption.

https://doi.org/10.1038/s41564-024-01794-8

Extended Data Fig. 5 | Candidalysin interacts with GAGs and their analogs. **a**, Transmission electron microscopic (TEM, top left) and atomic force microscopic (AFM, bottom left) images of candidalysin on a solid substrate with or without dextran, dextran sulfate and heparan sulfate. Scale bar: 200 nm. The right panel shows the number of loops per μm^2 in the AFM images from 3 independent experiments. **b**, Diagram illustrating the C-laurdan assay. **c**, Time course of the effects of dextran sulfate (50 μg/mL) on the GP score in the C-laurdan assay in the absence of candidalysin. Data are the mean ± SD of 3 experiments. **d**, Dextran sulfate (50 μg/mL) reduces the rate of candidalysin-induced membrane damage in POPC vesicles. Representative time course (left). Combined results from 4 experiments (right). The t_{50} represents the time when 50% membrane leakage occurred. Results are mean ± SD of 3 experiments. **e**, Comparison of the effects of a 6-h exposure to the indicated concentrations of candidalysin and CFSE-candidalysin on the survival (measured by an XTT assay) of TR146 cells. Results are mean ± SD of two experiments, each performed in triplicate. **f**, Colocalization analysis of heparan sulfate and CFSE-candidalysin on TR146 cells. Overlap coefficient R and Pearson's coefficient R(r) were generated by the Olympus software CellSens. Results are mean ± SD of 3 independent experiments, each quantifying 4 independent images. **g**, Damage (measure by an LDH assay) to TR146 and B3GAT3$^{-/-}$ cells caused by the *C. albicans ece1*Δ/Δ mutant (MOI = 5) after 5 h of infection. Results are mean ± SD of three experiments, each performed in triplicate. **h, i**, Effects of 100 μg/ml dextran and dextran sulfate on the number of cell-associated and endocytosed cells of the *C. albicans ece1*Δ/Δ mutant. The average number of organisms per high-power field that were associated with and endocytosed by TR146 cells were 8.81 ± 1.81 and 2.27 ± 1.31, respectively. P values were calculated using the unpaired, two-sided Student's t-test (**d, g**) and one way ANOVA with Dunnett's test for multiple comparisons (**a, e, h, i**).

https://doi.org/10.1038/s41564-024-01794-8

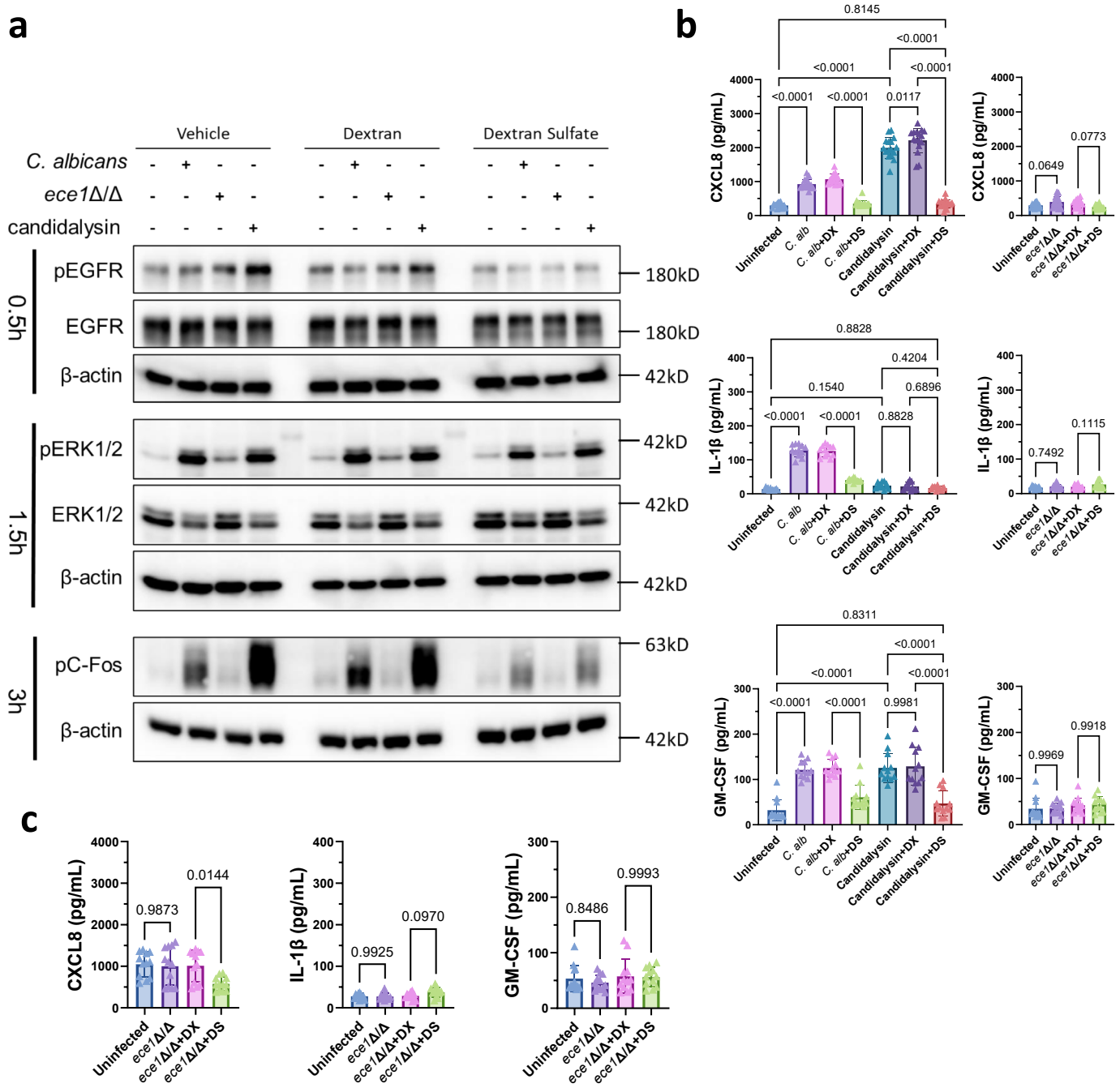

Extended Data Fig. 6 | Effects of dextran and dextran sulfate on stimulation of B3GAT3$^{-/-}$ cells by candidalysin and live *C. albicans*. **a**, Immunoblot showing the phosphorylation of the epidermal growth factor receptor (EGFR), extracellular regulated kinase1/2 (ERK1/2) and c-Fos transcription factor in B3GAT3$^{-/-}$ epithelial cells induced by wild-type *C. albicans* SC5314 (MOI = 5), the *ece1*Δ/Δ mutant, or candidalysin (10 µM) with or without dextran (DX) and dextran sulfate (DS) (100 µg/ml) at the time points indicated on the left. Shown are representative results of 3 independent experiments. **b**, The effects of dextran (DX) and dextran sulfate (DS) (100 µg/ml) on the production of CXCL8 (top), IL-1β (middle) and GM-CSF (bottom) by B3GAT3$^{-/-}$ cells incubated for 6 h with wild-type *C. albicans* (MOI = 5) or candidalysin (10 µM) (left panel) or infected with the *C. albicans* *ece1*Δ/Δ mutant (right panel). Results are mean ± SD of 3-4 experiments, each performed in replicates of 4. **c**, Effects of dextran and dextran sulfate (100 µg/ml) on the production of CXCL8, IL-1β, and GM-CSF by TR146 cells infected with the *ece1*Δ/Δ mutant (right, MOI = 5) for 6 h. Results are mean ± SD of 3 experiments, each performed in replicates of 4. P values were calculated using the one-way ANOVA with Dunnett's multiple comparisons test (**b-c**).

https://doi.org/10.1038/s41564-024-01794-8

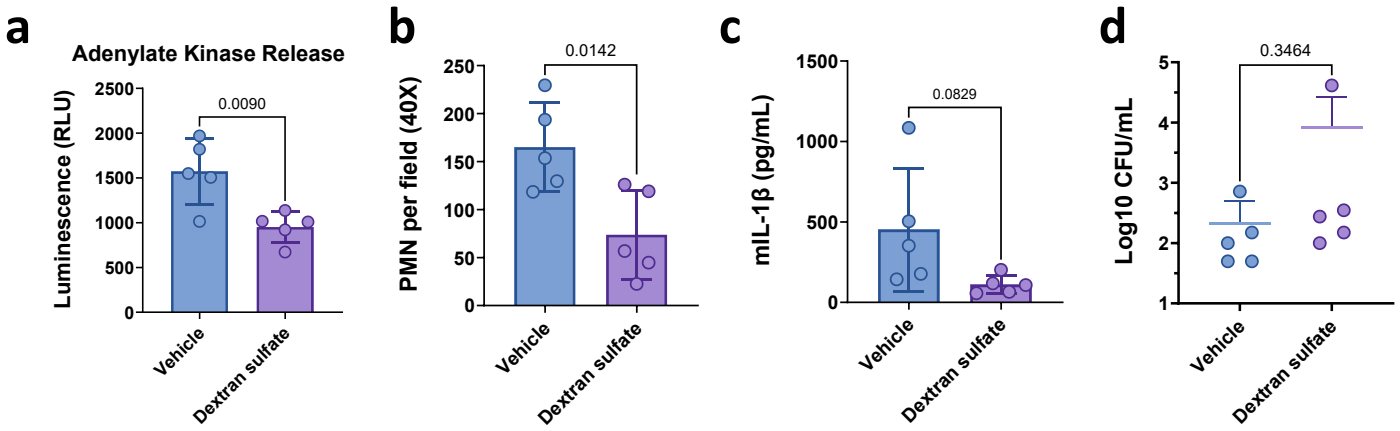

Extended Data Fig. 7 | Dextran sulfate protects vaginal epithelial cells from damage and inhibits pro-inflammatory cytokine production in CD-1 mice with vulvovaginal candidiasis. a-d, CD-1 mice were treated with either dextran sulfate or vehicle alone intravaginally prior to vaginal inoculation with wild-type *C. albicans* SC5314 and daily thereafter. After 3 days of infection, the concentration of adenylate kinase (a measure of host cell damage) (**a**), neutrophils (PMN) (**b**), IL-1β (**c**), and fungal colony forming units (CFU) (**d**) in the vaginal lavage fluid was determined. Results in (**a-d**) are the mean ± SD of 5 mice per experimental group in a single experiment. P values were calculated using the unpaired, two-sided student's t-test (**a-d**).

https://doi.org/10.1038/s41564-024-01794-8

Extended Data Table 1 | Sequences of oligonucleotides used for guide RNAs

Primer Sequence	Target Gene	Purpose
caccgCCAGAGCCCATACCTGGCAT	B3GAT3	B3GAT3_gRNA1-F
aaacATGCCAGGTATGGGCTCTGGc	B3GAT3	B3GAT3_gRNA1-R
caccgCGAGCTGTACCAGCGCGTAG	B3GAT3	B3GAT3_gRNA2-F
aaacCTACGCGCTGGTACAGCTCGc	B3GAT3	B3GAT3_gRNA2-R
caccgCGATGACAACACCTACAGCC	B3GAT3	B3GAT3_gRNA3-F
aaacGGCTGTAGGTGTTGTCATCGc	B3GAT3	B3GAT3_gRNA3-R
caccgGAGCCCATACCTGGCATAGG	B3GAT3	B3GAT3_gRNA5-F
aaacCCTATGCCAGGTATGGGCTCc	B3GAT3	B3GAT3_gRNA5-R
caccgCGTTAGATGCGCTGGACCCG	B3GAT3	B3GAT3_gRNA6-F
aaacCGGGTCCAGCGCATCTAACGc	B3GAT3	B3GAT3_gRNA6-R
caccgCGACGCCTACGAAAACCTCA	B3GALT6	B3GALT6_gRNA1-F
aaacTGAGGTTTTCGTAGGCGTCGc	B3GALT6	B3GALT6_gRNA1-R
caccgCGCCTTGAGCACGAACTCGA	B3GALT6	B3GALT6_gRNA2-F
aaacTCGAGTTCGTGCTCAAGGCGc	B3GALT6	B3GALT6_gRNA2-R
caccgTGCGGCCCGACATCGCCCTG	B3GALT6	B3GALT6_gRNA4-F
aaacCAGGGCGATGTCGGGCCGCAc	B3GALT6	B3GALT6_gRNA4-R
caccgCGCGGACCAGTCGTACACGT	B3GALT6	B3GALT6_gRNA5-F
aaacACGTGTACGACTGGTCCGCGc	B3GALT6	B3GALT6_gRNA5-R
caccgACACCTGGTTGGATAGTCAG	XYLT2	XYLT2_gRNA1-F
aaacCTGACTATCCAACCAGGTGTc	XYLT2	XYLT2_gRNA1-R
caccgCATGTAGGCGATTCGCACCG	XYLT2	XYLT2_gRNA3-F
aaacCGGTGCGAATCGCCTACATGc	XYLT2	XYLT2_gRNA3-R
caccgAAACACAATTAACTGGACAC	SLC39A9	SLC39A9_gRNA1-F
aaacGTGTCCAGTTAATTGTGTTTc	SLC39A9	SLC39A9_gRNA1-R
caccgATGTTGCTGGTGGACCAGAT	SLC39A9	SLC39A9_gRNA2-F
aaacATCTGGTCCACCAGCAACATc	SLC39A9	SLC39A9_gRNA2-R
caccgGACAACCAGACCCAGCGTGG	SLC39A9	SLC39A9_gRNA3-F
aaacCCACGCTGGGTCTGGTTGTCc	SLC39A9	SLC39A9_gRNA3-R
caccgAGCCTGTCATATGCCAGTGA	EMP1	EMP1_gRNA2-F
aaacTCACTGGCATATGACAGGCTc	EMP1	EMP1_gRNA2-R
caccgATACTCACAGCACACCAGTG	EMP1	EMP1_gRNA3-F
aaacCACTGGTGTGCTGTGAGTATc	EMP1	EMP1_gRNA3-R

nature portfolio

Corresponding author(s): Scott G. Filler

Last updated by author(s): Jul 1, 2024

Reporting Summary

Nature Portfolio wishes to improve the reproducibility of the work that we publish. This form provides structure for consistency and transparency in reporting. For further information on Nature Portfolio policies, see our Editorial Policies and the Editorial Policy Checklist.

Statistics

For all statistical analyses, confirm that the following items are present in the figure legend, table legend, main text, or Methods section.

n/a	Confirmed	
☐	☒	The exact sample size (*n*) for each experimental group/condition, given as a discrete number and unit of measurement
☐	☒	A statement on whether measurements were taken from distinct samples or whether the same sample was measured repeatedly
☐	☒	The statistical test(s) used AND whether they are one- or two-sided *Only common tests should be described solely by name; describe more complex techniques in the Methods section.*
☐	☒	A description of all covariates tested
☐	☒	A description of any assumptions or corrections, such as tests of normality and adjustment for multiple comparisons
☐	☒	A full description of the statistical parameters including central tendency (e.g. means) or other basic estimates (e.g. regression coefficient) AND variation (e.g. standard deviation) or associated estimates of uncertainty (e.g. confidence intervals)
☐	☒	For null hypothesis testing, the test statistic (e.g. *F*, *t*, *r*) with confidence intervals, effect sizes, degrees of freedom and *P* value noted *Give P values as exact values whenever suitable.*
☒	☐	For Bayesian analysis, information on the choice of priors and Markov chain Monte Carlo settings
☒	☐	For hierarchical and complex designs, identification of the appropriate level for tests and full reporting of outcomes
☐	☒	Estimates of effect sizes (e.g. Cohen's *d*, Pearson's *r*), indicating how they were calculated

Our web collection on statistics for biologists contains articles on many of the points above.

Software and code

Policy information about availability of computer code

Data collection	N/A
Data analysis	Graphpad Prism, version 10 CellSens Olympus microscope software, version 3.1(build 21199)

For manuscripts utilizing custom algorithms or software that are central to the research but not yet described in published literature, software must be made available to editors and reviewers. We strongly encourage code deposition in a community repository (e.g. GitHub). See the Nature Portfolio guidelines for submitting code & software for further information.

Data

Policy information about availability of data

All manuscripts must include a data availability statement. This statement should provide the following information, where applicable:

- Accession codes, unique identifiers, or web links for publicly available datasets
- A description of any restrictions on data availability
- For clinical datasets or third party data, please ensure that the statement adheres to our policy

The original sequencing data were deposited to the NCBI under BioProject PRJNA1081917. All data from this study are presented in the manuscript and Extended Data figures and tables.

Research involving human participants, their data, or biological material

Policy information about studies with human participants or human data. See also policy information about sex, gender (identity/presentation), and sexual orientation and race, ethnicity and racism.

Reporting on sex and gender	Not applicable
Reporting on race, ethnicity, or other socially relevant groupings	*Please specify the socially constructed or socially relevant categorization variable(s) used in your manuscript and explain why they were used. Please note that such variables should not be used as proxies for other socially constructed/relevant variables (for example, race or ethnicity should not be used as a proxy for socioeconomic status).* *Provide clear definitions of the relevant terms used, how they were provided (by the participants/respondents, the researchers, or third parties), and the method(s) used to classify people into the different categories (e.g. self-report, census or administrative data, social media data, etc.)* *Please provide details about how you controlled for confounding variables in your analyses.*
Population characteristics	*Describe the covariate-relevant population characteristics of the human research participants (e.g. age, genotypic information, past and current diagnosis and treatment categories). If you filled out the behavioural & social sciences study design questions and have nothing to add here, write "See above."*
Recruitment	*Describe how participants were recruited. Outline any potential self-selection bias or other biases that may be present and how these are likely to impact results.*
Ethics oversight	*Identify the organization(s) that approved the study protocol.*

Note that full information on the approval of the study protocol must also be provided in the manuscript.

Field-specific reporting

Please select the one below that is the best fit for your research. If you are not sure, read the appropriate sections before making your selection.

☒ Life sciences ☐ Behavioural & social sciences ☐ Ecological, evolutionary & environmental sciences

For a reference copy of the document with all sections, see nature.com/documents/nr-reporting-summary-flat.pdf

Life sciences study design

All studies must disclose on these points even when the disclosure is negative.

Sample size	In the mouse vulvovaginitis experiments, we planned to study a continuous response variable (vaginal adenylate kinase release) from independent control and experimental mice with 1 control per experimental animal. In our previous studies, the response to C. albicans within each subject group was normally distributed with a standard deviation of 25%. If the true difference in the experimental and control means is 40%, we will need to study 6 experimental subjects and 6 control subjects to be able to reject the null hypothesis that the population means of the experimental and control groups are equal with probability (power) of 0.8. The Type I error probability associated with this test of the null hypothesis is 0.05. For the in vitro experiments, we planned to study a continuous response variable (epithelial cell damage, invasion, or adherence from independent control and experimental groups with 1 control per experimental group. In our previous studies, the response to C. albicans within each subject group was normally distributed with a standard deviation of 25%. If the true difference in the experimental and control means is 35%, we will need to study 8 experimental subjects and 8 control subjects to be able to reject the null hypothesis that the population means of the experimental and control groups are equal with probability (power) of 0.8. The Type I error probability associated with this test of the null hypothesis is 0.05.
Data exclusions	2 B6 mice (one in each experimental group) was excluded from the C. albicans vulvovaginitis study because it had an extremely low fungal burden, indicating that it was not adequately estrogenized. In the CD-1 mouse experiment, 16 mice per treatment group were treated with estrogen and infected with C. albicans, but only 5 mice per group had detectable C. albicans counts in their vaginal lavage (consistent with the known resistance of this mouse strain to vaginal candidiasis). The 11 mice per group without candidal vaginitis were excluded from the analysis.
Replication	All experiments were performed at least twice and most were performed three or four times.
Randomization	Mice were randomly selected to the two treatment groups. Samples were allocated randomly for treatments (untreated, infected etc.).
Blinding	The investigators were not blinded to the treatment of the mice because the treatment outcomes were objective, not subjective.

Reporting for specific materials, systems and methods

We require information from authors about some types of materials, experimental systems and methods used in many studies. Here, indicate whether each material, system or method listed is relevant to your study. If you are not sure if a list item applies to your research, read the appropriate section before selecting a response.

Materials & experimental systems

n/a	Involved in the study
☐	☒ Antibodies
☐	☒ Eukaryotic cell lines
☒	☐ Palaeontology and archaeology
☐	☒ Animals and other organisms
☒	☐ Clinical data
☒	☐ Dual use research of concern
☒	☐ Plants

Methods

n/a	Involved in the study
☒	☐ ChIP-seq
☐	☒ Flow cytometry
☒	☐ MRI-based neuroimaging

Antibodies

Antibodies used: mouse anti-Cas9 (Santa Cruz, #sc517386, lot H1420; 1:100 dilution), mouse anti-hGBF1 (Santa Cruz, #sc136240, lot E0820; 1:100 dilution), mouse anti-c-Fos (Santa Cruz, #sc8047), mouse anti-hB3GAT3 (Santa Cruz, #sc390526, lot D2513; 1:100 dilution), mouse anti-hXYLT2 (Santa Cruz, #sc374134, lot H2611; 1:100 dilution), mouse anti-b-actin (Santa Cruz, C4, #sc47778, lot G1223; 1:100 dilution), mouse anti-Heparan Sulfate antibody (AMSBIO, clone F58-10E4, #3702551), rabbit anti-phospho-c-Fos (Cell Signaling, Ser32, #5348, lot 4; 1:1000 dilution), rabbit anti-phospho-EGFR (Cell Signaling, Tyr1068, #2234; 1:1000 dilution), rabbit anti- EGFR (Cell Signaling, #4267; 1:1000 dilution), rabbit anti-phospho-ERK1/2 (Cell Signaling, Thr202/Tyr204, #4370; 1:1000 dilution), rabbit anti-ERK1/2 (Cell Signaling, #4695; 1:1000 dilution), rabbit anti-GAPDH (Cell Signaling, #5174; 1:3000 dilution), Rabbit anti-hB3GALT6 (ProteinTech, #55049-1-AP), rabbit anti-hSLC39A9 (Invitrogen, #PA5-75557), rabbit anti-EMP1 (Bioss Antibodies, #bs-0558r), Cross-adsorbed goat anti-mouse IgG-HRP (Invitrogen, #G21040), goat anti-rabbit IgG-HRP(Invitrogen, #G21234) and goat anti-mouse IgM-Alexa568 (Invitrogen, #A21043)

Validation: The antibodies were validated by the the manufacturers.

Eukaryotic cell lines

Policy information about cell lines and Sex and Gender in Research

Cell line source(s): The TR146 oral epithelial cell line was originally from a female with oral cancer
The A431 vaginal epithelial cell line was from a female.
The HEK-293T cell line was from a female.

Authentication: None of the cell lines used were authenticated.

Mycoplasma contamination: The cell lines were not tested for mycoplasma contamination

Commonly misidentified lines (See ICLAC register): None

Animals and other research organisms

Policy information about studies involving animals; ARRIVE guidelines recommended for reporting animal research, and Sex and Gender in Research

Laboratory animals: 6-8-week-old female C57BL/6 and CD-1 mice. Mice were kept in specific pathogen-free facilities, following a 12-hour light/12-hour dark cycle, and has as libitum access to food and water. Food and water were provided ad libtum.

Wild animals: Not applicable.

Reporting on sex: Only female mice were used because we were studying vaginal infection.

Field-collected samples: Not applicable.

Ethics oversight: The animal work conducted in this study was approved by the UTHSC Institutional Animal Care and Use Committee under protocol 21-0265 in accordance with the Guide for the Care and Use of Laboratory Animals

Note that full information on the approval of the study protocol must also be provided in the manuscript.

Plants

Seed stocks	*Report on the source of all seed stocks or other plant material used. If applicable, state the seed stock centre and catalogue number. If plant specimens were collected from the field, describe the collection location, date and sampling procedures.*
Novel plant genotypes	*Describe the methods by which all novel plant genotypes were produced. This includes those generated by transgenic approaches, gene editing, chemical/radiation-based mutagenesis and hybridization. For transgenic lines, describe the transformation method, the number of independent lines analyzed and the generation upon which experiments were performed. For gene-edited lines, describe the editor used, the endogenous sequence targeted for editing, the targeting guide RNA sequence (if applicable) and how the editor was applied.*
Authentication	*Describe any authentication procedures for each seed stock used or novel genotype generated. Describe any experiments used to assess the effect of a mutation and, where applicable, how potential secondary effects (e.g. second site T-DNA insertions, mosiacism, off-target gene editing) were examined.*

Flow Cytometry

Plots

Confirm that:

☒ The axis labels state the marker and fluorochrome used (e.g. CD4-FITC).

☒ The axis scales are clearly visible. Include numbers along axes only for bottom left plot of group (a 'group' is an analysis of identical markers).

☒ All plots are contour plots with outliers or pseudocolor plots.

☒ A numerical value for number of cells or percentage (with statistics) is provided.

Methodology

Sample preparation	To measure calcium flux, TR146 cells and B3GAT3-/- cells at 1 million cells/ml were loaded with the calcium probe Indo-1/AM (4 µM, Biotium, #500431) for 30 min at 37°C in cell loading medium (CLM, DMEM/F12+ 2% heat-inactivated fetal bovine serum + 25 mM HEPES) containing 1 mM EGTA. Cells were washed twice and kept at 37°C in CLM at a concentration of 1× 106 cells/mL for another 30 minutes before flow cytometry. Calcium flux measurements were performed on a FACSymphony™ A5 cytometer (BD Biosciences) as suggested by the manufacture. After a baseline Indo-1 fluorescence was recorded for 90 sec, cells were treated with 1 µM of calcium ionophore A23187 (Sigma Aldrich, #C7522) or 10 µM of candidalysin while cell acquisition continued. Acquisition was performed for additional 6 min after treatment. The calcium flux was calculated as the ratio of fluorescence intensity at 395nm (Ca2+-bound) and 496nm (Ca2+-free), and followed over time. A kinetic analysis was performed using FlowJo software and the normalized (to the baseline) smoothed means of fluorescence ratios were plotted. To quantify the levels cell surface heparan sulfate, 1 million of TR146, XYLT2-/-, B3GALT6-/- and B3GAT3-/- cells were fixed with 4% of paraformaldehyde for 10 min, and then blocked with 5% goat serum for 30 min before a 1-h incubation with a primary anti-heparan sulfate antibody (clone F58-10E4, #3702551) at 1:100 in FACS buffer (PBS + 5% FBS). After washing 3 times with FACS buffer, cells were incubated with goat anti-mouse IgM-Alexa633 (#A21046) at 1:100 in FACS buffer for 1 h. Cell surface heparan sulfate was quantified using a FACSymphony™ A5 cytometer and the results were analyzed with FlowJo software.
Instrument	FACSymphony™ A5 cytometer
Software	FlowJo V10
Cell population abundance	TR146, XYLT2-/-, B3GALT6-/-, AND B3GAT3-/- cells(50000 counts) were used for cell surface heparan sulfate analysis. For calcium influx assay, total of 10 minutes counting with no specific total cell number.
Gating strategy	Gating based on cell size (FSC and SSC) for heparan sulfate staining, and additional gating of fluorencence intensity at 395nm and 496nm for calcium influx assay. Gating strategy provided in the source data.

☒ Tick this box to confirm that a figure exemplifying the gating strategy is provided in the Supplementary Information.